Review of Materials Research 1 (2025) 100014

Contents lists available at ScienceDirect

Review of Materials Research

journal homepage: www.sciencedirect.com/journal/review-of-materials-research

Progress of copper-based friction materials for high-speed train: Tribological property involving components, interfaces, and tribo-layers

Yuxuan Xu [a], Haibin Zhou [b], Qi Chen [a], Donglin Liu [a], Yong Han [a], Minwen Deng [a], Pingping Yao [a,*]

[a] State Key Laboratory of Powder Metallurgy, Central South University, Changsha, 410083, China
[b] Hunan Province Key Laboratory of Materials Surface/Interface Science & Technology, Central South University of Forestry and Technology, Changsha, 410004, China

ARTICLE INFO

Keywords:
Copper-based friction materials
High-speed train brake
Tribological property
Components
Interfaces
Tribo-layers

ABSTRACT

With the continuous increase in operating speed of high-speed trains, enhanced safety and stability in braking systems are necessitated. Copper-based friction materials (CBFMs) are predominantly utilized in brake pads for high-speed trains exceeding 300 km/h. Substantial braking energy is dissipated by CBFMs through direct interaction with counterpart materials, and their pivotal role in maintaining the safety and reliability of high-speed braking systems is ensured. The components and intrinsic properties, the multiple variations at the interface, and the distinctive characteristics of brake conditions are regarded as the primary factors influencing the braking properties of CBFMs. Recent advancements in CBFMs and tribological properties are systematically explored in this review from three critical perspectives: components, interfaces, and tribo-layers. Firstly, the emerging trends in matrix, lubricant components, and abrasive components in CBFMs are detailed. Secondly, the correlation between interfacial and tribological properties at both micro and macro scales is investigated. Thirdly, the characteristics of tribo-layers at different scales and the associated wear mechanisms of CBFMs are examined. Lastly, the challenges CBFMs face and the constraints of multi-component synergistic design, evaluation methodologies, and novel wear mechanisms are highlighted.

1. Introduction

High-speed trains are defined as trains traveling at speeds exceeding 200 km/h and are renowned for their rapid transportation, safety, and large passenger capacity. In China, operating speed exceeding 300 km/h has been achieved, with future targets aiming to surpass 400 km/h. These advancements pose significant challenges for the braking systems of high-speed trains [1–3]. The braking system, comprising brake pads and their counterpart brake discs, plays a pivotal role in ensuring the emergency braking properties and operational safety of high-speed trains (Fig. 1a and b) [4,5]. At present, copper-based friction materials (CBFMs) fabricated through powder metallurgy are predominantly utilized in brake pads of high-speed trains exceeding 300 km/h, characterized by a stable coefficient of friction (COF), superior wear resistance, outstanding thermal stability, and excellent mechanical strength (Fig. 1c and d) [6,7]. Significantly, the surfaces of brake pads and discs endure repeated high-temperature, high-pressure thermal shocks [8,9]. With the continuous increase in the operating speed of high-speed trains, CBFMs encounter challenges, including reduced braking efficiency and abnormal wear growth, highlighting the urgent need to develop CBFMs capable of meeting stricter property requirements.

Three key factors govern the braking properties of CBFMs: (i) the material components and intrinsic properties, encompassing the design of the matrix, abrasive components, and lubricant components; (ii) the interfacial interactions and damage mechanisms between the matrix and its components, alongside the formation and damage processes of the tribo-layers; and (iii) the operational behavior of CBFMs in open braking systems and under complex environmental conditions, mated with advancements in counterpart materials. This review provides a comprehensive investigation of CBFMs for high-speed trains, examining them from three critical perspectives: components, interfaces, and tribo-layers. Meanwhile, the primary challenges these CBFMs face are identified, and forward-looking perspectives on future development trends are offered, with the aim of supporting the innovation and application of next-generation CBFMs with better properties.

* Corresponding author.
E-mail address: ppyao@csu.edu.cn (P. Yao).

https://doi.org/10.1016/j.revmat.2025.100014
Received 21 March 2025; Received in revised form 5 April 2025; Accepted 6 April 2025
Available online 8 April 2025

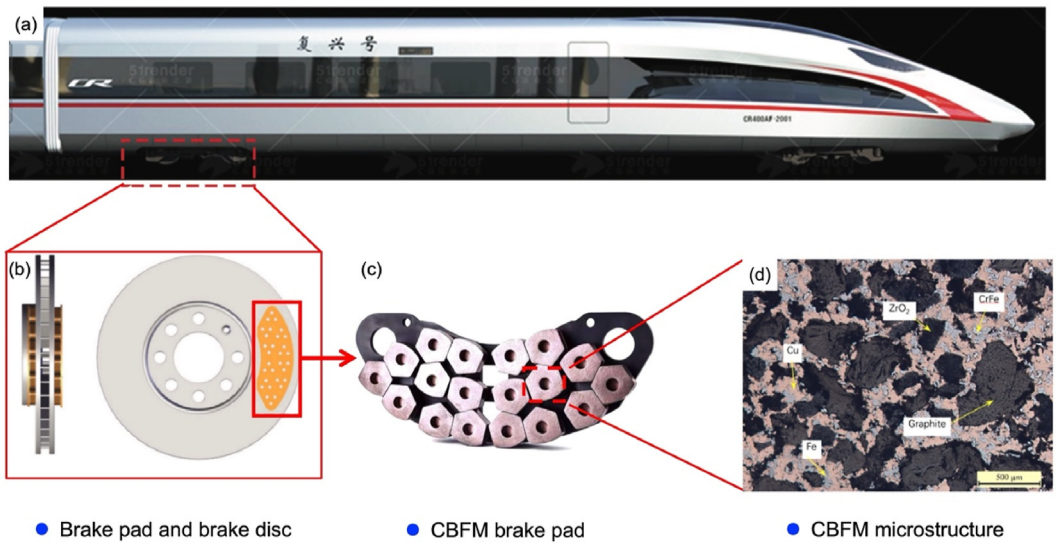

Fig. 1. High-speed train braking systems and CBFM. (a) High-speed train; (b) high-speed train brake pads, and brake disc; (c) CBFM brake pad; (d) CBFM material microstructure. Taken from Refs. [4–6] with permission.

2. Components

CBFMs are composite materials fabricated via powder metallurgy, comprising a copper matrix reinforced with different components. Based on their functional roles in braking process, the components of CBFMs can be categorized as the matrix, abrasive components, and lubricant components (Fig. 2). The abrasive components ensure a high COF and excellent wear resistance, whereas the lubricant components provide lubrication and contribute to COF stability. Hence, the selection and composition of raw powders directly impact the properties. The components of CBFMs allow for flexible adjustment and slight variations. The design and regulation of components significantly influence the microstructure, property, and reliability. Achieving low-cost, high-property CBFMs through component regulation is a shared goal among researchers.

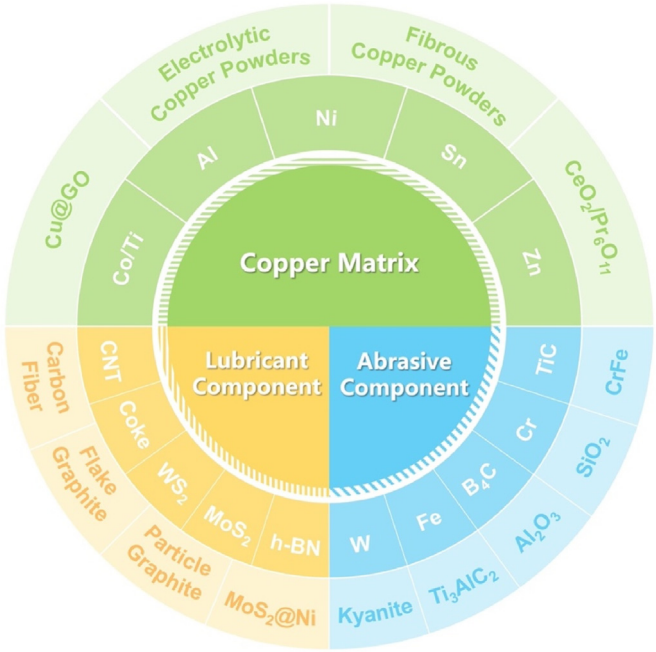

Fig. 2. Three types of components in CBFMs.

2.1. Matrix

As the fundamental component of CBFMs, copper powder constitutes approximately 50 wt% of the total powder mass, significantly influencing the braking property. The unique dendritic morphology and inherent deformability of electrolytic copper powder impart remarkable mechanical properties and optimal braking performance to CBFMs, establishing it as the primary powder utilized in CBFMs (Fig. 3a) [6,10,11]. Analyses of the physical parameters of copper powder reveal that increased complexity and irregularity of copper powder morphology correlate with enhanced mechanical properties in CBFMs. A cyclic oxidation and fiber grinding strategy to prepare fibrous copper powder with a fibrous morphology has been reported. As shown in Fig. 3b, the incorporation of fibrous copper powder into CBFMs markedly enhances the stability of the COF and wear resistance, compared to electrolytic copper powder [12].

To concurrently enhance the mechanical, and wear resistance properties of CBFMs, additional metal components are often introduced to strengthen the matrix. The addition of Ni and Sn elements facilitates solid solution and dispersion strengthening within the copper matrix, thereby improving braking properties at high temperatures. Given their similar atomic scale, Ni atoms can diffuse within the copper matrix, forming an unlimited substitutional solid solution, which contributes to solid-solution strengthening [13]. While the incorporation of Ni enhances the hardness of both the matrix and the tribo-layer, it paradoxically results in increased wear due to a reduction in the plasticity of the worn surface, subsequently causing extensive spalling pits (Fig. 3c). Sn and Zn are often introduced in the form of bronze powder, the addition of Sn promotes liquid-phase sintering, enhancing material density; however, excessive Sn can lead to a decrease in the COF and cause plastic deformation damage. Compared to Sn and Zn, Al exhibits a more pronounced strengthening effect on the copper matrix, with Cu-Al alloys showing superior overall physical and mechanical properties compared to Cu-Sn/Zn alloys. Furthermore, CBFMs containing Al demonstrate enhanced heat resistance and corrosion resistance [14]. Additionally, the synergistic interaction between Sn and Ni results in remarkable property enhancements. As illustrated in Fig. 3d, the CBFM incorporating both Ni and Sn maintains a high and stable COF across the temperature range of 100–300 °C.

Copper surface coating is another strategy to reinforce the matrix, by coating copper powder (Cu@GO) with graphene oxide and preparing Cu@GO-enhanced CBFM, we have demonstrated that the introduction of

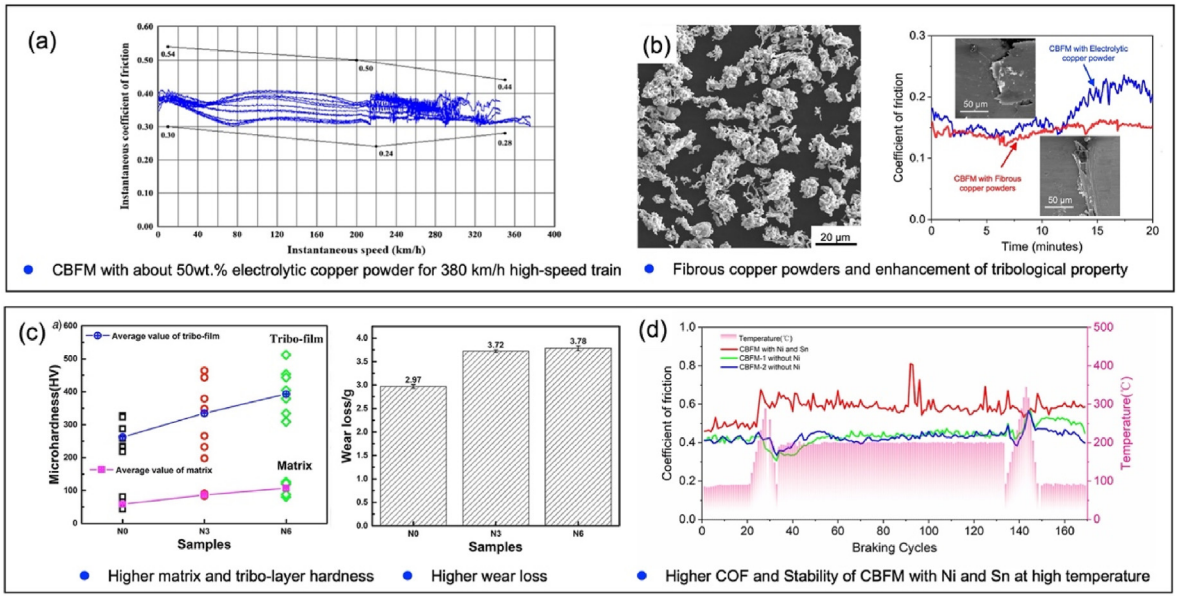

Fig. 3. Tribological property of CBFMs with matrix and strength components. (a) Electrolytic copper powder. (b) Fibrous copper powders. (c) Ni powders. (d) Ni and Sn powders. Taken from Refs. [6,12,13] with permission.

Cu@GO enables CBFM to sustain greater braking energy and effectively mitigates worn surface damage. This process achieves uniform dispersion of graphene within CBFM, significantly enhancing thermal conductivity and mechanical properties [15]. The addition of trace metal elements, such as Co and Ti, can modulate the Cu/C interface structure, significantly enhancing interfacial bonding strength between components and improving tribological property [16,17]. Recently, enhancement of brake properties (wear loss $<2.5 \times 10^{-7}$ g/J) under heavy load by incorporating CeO_2 and Pr_6O_{11} were reported [18,19]. These emerging components have significantly advanced the microstructural characteristics of the CBFM matrix, however, forming a stable modified copper metal structure in multi-component systems remains challenging, for instance, the high cost of transition metals limits their use in cost-sensitive CBFMs. In conclusion, matrix-strengthening components synergistically enhance the mechanical and tribological properties of CBFMs, offering considerable potential for designing toughened materials. Furthermore, modifications in copper are pivotal, as they profoundly influence adhesion to counterpart materials, material cohesion, and the capacity to bear overall braking energy.

2.2. Abrasive components

Abrasive components typically consist of hard particles, including various metals, metal oxides, and carbides, which serve to stabilize the COF and to ensure reliability during high-speed, high-temperature braking. Present research on abrasive components mainly investigates microscopic interfacial bonding and the evolution of particle behavior under high-speed, high-temperature operating conditions. Fe is extensively utilized in CBFMs, where an increased Fe content not only ensures a higher COF but also enhances the uniformity, density, and continuity of the oxide film on friction surfaces [20,21]. Peng et al. observed that raising the relative Fe content accelerates the formation rate of the surface oxide layer during high-speed braking, facilitating a more continuous and stable oxide layer and contributing to a more stable COF and reduced wear loss [22]. However, an excessively high content may weaken adhesion to the substrate, causing abnormal spalling, to optimize its reinforcing effect, the Fe content is controlled at approximately 20 wt % of the total powder mass. Furthermore, surface modification of Fe powder can enhance braking properties. Carbonyl iron powder effectively increases the hardness and deformation resistance of the tribo-layer, while supporting the tribo-layer within the substrate, thereby improving braking properties under high-speed conditions [23–25].

Cr, CrFe, SiC, SiO_2, Al_2O_3, ZrO_2, and TiC are frequently utilized as abrasive components in CBFMs and have found extensive application in high-speed train braking systems [26–28]. Studies reveal that despite Cr exhibiting greater hardness than Fe, CBFMs incorporating Cr may still cause damage to counterpart materials. The synergistic strengthening effect of CrFe particles surpasses that of Cr or Fe individually, with the addition of trace amounts significantly enhancing both the COF and braking stability. Currently, high-strength Cr-Fe alloys have largely replaced Cr particles and are extensively utilized in the CBFM [27]. Incorporating ceramic particles, including silicon carbide (SiC) and aluminum oxide (Al_2O_3), significantly enhances wear resistance under elevated temperatures and high-speed conditions. SiC particles, known for their high hardness, are especially suitable for high-speed applications [29,30]. Zhang et al. found that under high-speed braking, copper-coated SiO_2 exhibits stronger interfacial bonding with the matrix [31]. Materials containing copper-coated SiO_2 show higher and more stable COFs, with reduced COF decay. Si et al. found that SiO_2, Al_2O_3, and SiC significantly enhance and stabilize braking properties at 500 °C [32]. Under high-temperature braking, CBFMs with TiC showed 60 % less wear compared to those with Al_2O_3, and exhibited more stable COFs. This is attributed to the lower thermal expansion coefficient of TiC, which reduces thermal stress at the interface with the matrix [33].

Certain natural ceramic powders exhibit multi-element composite structures. Unlike previously reported mineral powders, such as mullite over the past few decades, new ceramic powders are gradually explored for potential function. The kyanite ($Al_2(SiO_4)O$) promotes the formation of tribo-layers and oxide films, resulting in a dual-layer structure that stabilizes the COF [30]. Sepiolite and its modified particles have recently been reported as a new ceramic component, exhibiting wear resistance and high-temperature lubrication during the braking process, which can be ascribed to the Cu_2O, Fe_2O_3, and CaO metal films, while the internal layer consists of B_2O_3 film, graphite, and sepiolite (Fig. 4a and b) [34–36]. In addition to natural composite ceramic powders, composite ceramic powders are prepared, TiC-B_4C composite ceramic powder reinforcement improved the microhardness of the tribo-layer in CBFM, preventing further oxidation and corrosion [37]. B_4C-SiC composite ceramic powder reinforcement provided a high COF and friction stability, forming a friction film with high and wide-ranging microhardness

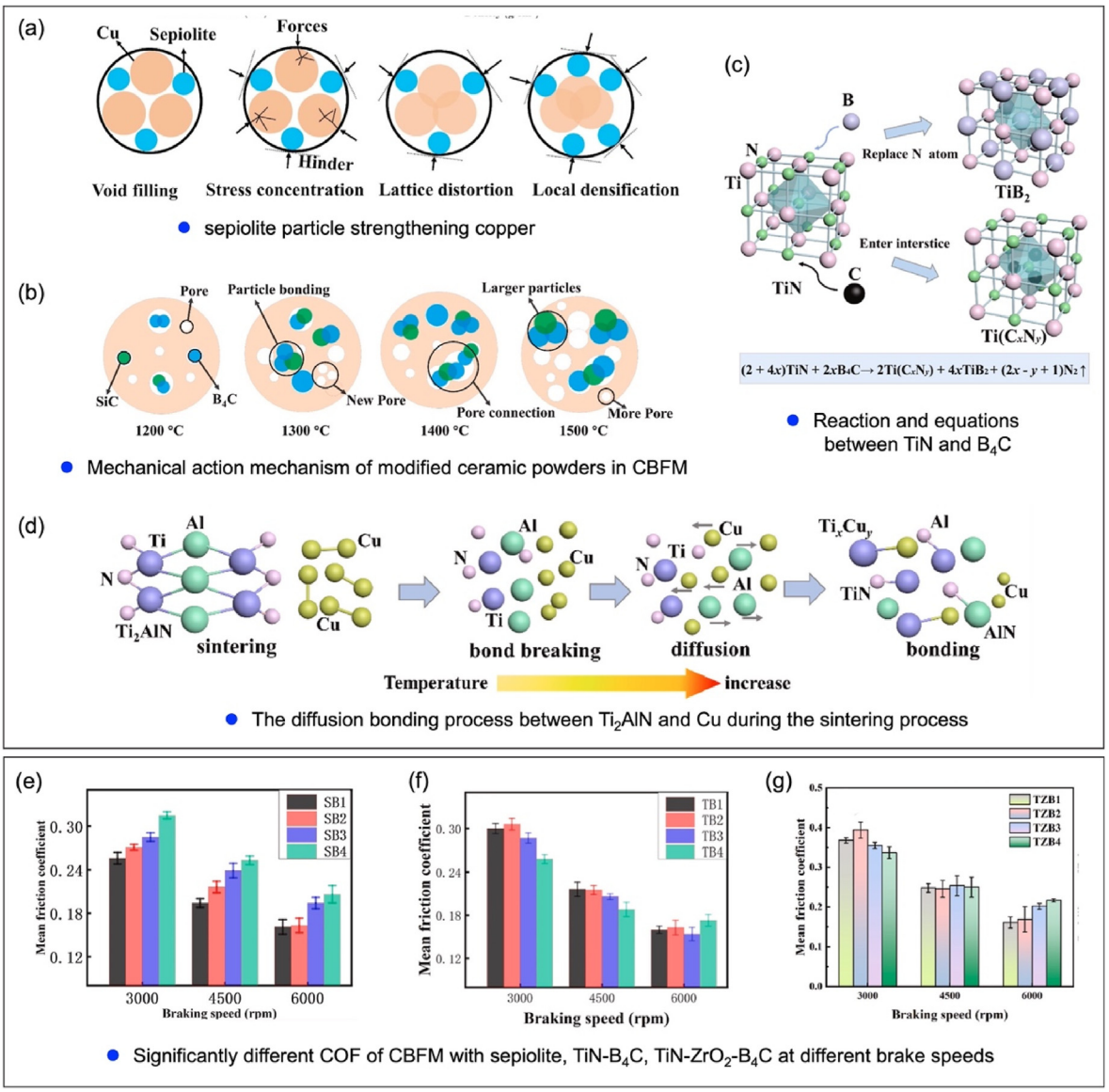

Fig. 4. Ceramic abrasive components and their effects on the brake properties of CBFMs. (a) Strengthening mechanism of sepiolite in copper base. (b) Action mechanism of modified ceramic powders. (c) Reaction process of TiN and B_4C. (d) Bonding process between Ti_2AlN and Cu. (e–g) COF of CBFMs with sepiolite, TiN-B_4C, Ti_2ALN-ZrO_2-B_4C at different brake speeds. Taken from Refs. [34,37–39,45,46] with permission.

[38,39] The synergistic effect of B_4C with components such as TiC, SiC, and ZrO_2 in CBFMs demonstrates that the synergistic effect formation of a B_2O_3 and metal can stabilize the braking process (Fig. 4c) [40].

$M_{n+1}AX_n$, a family of ternary layered ceramics, where M is an early transition metal, A is an A-group element (IIIA and IVA), and X is C and/or N with $n = 1–3$, for example, Ti_2AlN can enhance the braking property of CBFMs through their tribo-layers and tribo-oxidation (Fig. 4d). However, weak interfacial bonding and detachment under stress can cause third-body abrasion, increasing wear on both the CBFM and its counterpart during sliding [41–43]. Some approaches have been suggested to address these challenges, including the establishment of a strong bonding interface between the metal matrix and $M_{n+1}AX_n$ reinforcements, and the addition of robust ceramic particles like ZrO_2 to bear loads and limit deformation and microfracture of $M_{n+1}AX_n$ [44–46]. The core-shell structured graphene oxide-Ti_3AlC_2 ($M_{n+1}AX_n$) fabricated via liquid phase method and electroless plating method, contributes to improved wear resistance [47].

Both natural and composite ceramics demonstrate remarkable properties. However, under high-speed conditions, composite ceramic powder-reinforced CBFM exhibited a low COF (less than 0.2), in contrast to low-speed conditions (greater than 0.3), attributed to the excessive macro hardness and the high-temperature oxidation strengthening effect of the ceramic phase (Fig. 4e–g). The validation of these novel components remains relatively constrained, necessitating further exploration to assess their universality and broader applicability. The exploration of component content is a recurring theme in nearly all studies on component design. However, aside from adjusting the relative proportions of the matrix and variable components, research on the synergistic interactions among multiple components remains scarce despite its critical importance.

2.3. Lubricant components

Lubricant components are typically substances that possess lubricating properties, effectively reducing wear loss, enhancing braking stability, and minimizing noise. Common lubricant components include layered-structure materials such as graphite, molybdenum disulfide (MoS_2), hexagonal boron nitride (h-BN), and other substances exhibiting

similar structural characteristics, facilitating a stable and optimal COF (Table 1).

Graphite and MoS_2 are recognized for their ability to form effective lubricating films during frictional processes due to their excellent layered structures. Zhang et al. reported that flake graphite acts as a lubricant but does not contribute to forming a stable, continuous structure; in contrast, granular graphite behaves like hard particles on the friction surface, offering minimal lubrication [48]. Despite the inherent non-wettability of graphite with copper and its tendency to induce delamination and microcracks, it demonstrates exceptional thermal stability and promotes the formation of a carbonaceous layer at the friction interface, thereby often constituting a substantial volume fraction [6,21]. In comparison to graphite, coke possesses superior strength and a more intricate chemical composition, enhancing its interfacial adhesion with metals and promoting the stabilization of surface metal oxide layers. In addition, coke can enhance and stabilize the COF and reduce wear rate, although it cannot fully substitute for graphite [49]. The fine mosaic structure of coke demonstrates significant advantages in enhancing the braking stability and wear resistance of CBFMs [50,51]. Additionally, adding a small amount of artificial graphite can maintain matrix continuity while improving strength through partial carbide formation, thereby enhancing tribological property during high-speed emergency braking [52]. Zhang et al. indicated that copper-coated graphite particles can significantly enhance the interfacial bonding strength between copper and graphite, and reduce wear rate, demonstrating the efficacy of the coating process in strengthening interfacial adhesion [53]. However, compatibility of graphite with other components is limited, with mechanical damage predominantly occurring at the copper/carbon non-wetting interface, where crack initiation and propagation lead to material spalling and detachment. Graphite faces challenges in sustained use above 400 °C, as oxidation and ablation under high-energy braking reduce its lubricating effect. Enhancing the bonding strength between graphite and other components and improving its oxidation resistance is essential.

The mechanism of MoS_2 differs substantially from that of graphite. Zhang et al., through high-energy braking property analysis of CBFMs with varying MoS_2 contents, observed that adding an optimal amount of MoS_2 notably strengthens the tribo-layer and reduces material transfer on the friction surface, thereby stabilizing the COF under high-temperature conditions [54]. During high-speed emergency braking, MoS_2-containing materials form a vortex-structured tribo-layer on the surface, where rapid internal deformation and flow reduce the COF. However, when MoS_2 content is excessive, the tribo-layer becomes more susceptible to delamination, and the generated hard particles can compromise the tribo-layer, resulting in increasing wear. Ni coating MoS_2 can improve bonding with copper, showing the optimum performance in mechanical properties and lubricant behaviors, which exhibits potential application in CBFMs [55].

Table 1
COF and wear mechanisms of CBFMs with different lubricant components.

Lubricant components (wt%)					COF	Wear mechanism	
Graphite	Coke	MoS_2	h-BN	CF			
19		2			0.25–0.40	Delimination	[6]
10–18		5			0.23–0.32	Microcracks	[18]
10		5			0.31–0.42	Flocullent area	[21]
20					0.45–0.56	on interfaces	[23]
25–30		3–4			0.24–0.42	Covered carbon	[33]
5–10		1–5			0.31–0.40	layer	[24]
0–9	0–9	2			0.40–0.70	Limited plastic	[50]
10–20	0–10	2			0.20–0.35	deformation	[51]
9–18	0–9				0.24–0.31	Metal oxide layer	[52]
12			0–6		0.11–0.23	Anti-oxidation	[57]
10		2		1.2	0.28–0.45	Inhibiting plastic deformation	[59]

Hexagonal boron nitride (h-BN) exhibits a high oxidation temperature (900 °C) and remains stable during the sintering process [56], making it highly suitable for high-temperature service conditions. Chen et al. observed that adding 2 wt% h-BN enhances the COF, achieving high and stable levels [57]. However, at concentrations of 4 wt% and 6 wt%, the COF exhibits a significant decrease followed by an increase, which appears to be related to the interactions between Cu and Fe, though this phenomenon has not been fully explained. As for other materials featuring layered structures, tungsten disulfide (WS_2) is another high-temperature-resistant lubricating component, showing significant potential to enhance wear resistance and to lower the COF [58]. In addition, Zhang et al. observed that a 0.4 wt% nano carbon fiber in a CBFM, under high-energy braking conditions, forms a tribo-layer with cementite, featuring high resistance to plastic deformation, effectively reducing wear rate and maintaining COF stability [59].

The synergistic effects of multi-phase lubricant composite additives have been observed to significantly improve friction and wear properties. Numerous studies indicate that the combination of different lubricating phases can produce a synergistic effect, thereby further enhancing the overall property of CBFMs [60]. Guo et al. emphasized the microscopic friction mechanisms involved in lubricating film formation, supporting further exploration in multi-lubricant phase composite research [61]. At elevated temperatures, the tribo-layer of CBFM is highly prone to oxidation, resulting in the loss of lubricating films and instability in the COF. Therefore, enhancing the oxidation resistance of lubricating phases such as graphite is crucial for improving high-temperature stability of CBFMs [62]. In addition, the combination of MoS_2, WS_2, and h-BN shows that an optimal ratio can significantly enhance the wear resistance of CBFMs, indicating that these solid lubricants have considerable potential for oxidation-resistant applications [63–65].

Under high-speed braking conditions, characterized by high-pressure and high-temperature thermo-mechanical coupling, the strength of CBFMs and its capacity for thermal energy absorption play a pivotal role in determining its braking performance and operational lifespan. The influence of constituent components on the mechanical and thermal properties of CBFMs is highly pronounced. Table 2 lists the hardness, thermal conductivity, COF, and wear rates of various CBFM formulations across different braking speeds. Establishing a direct relationship between hardness or thermal conductivity and braking performance is inherently

Table 2
Hardness, thermal conductivity, and brake properties of CBFMs.

Hardness (HB)	Thermal conductivity ($W \cdot m^{-1} \cdot K^{-1}$)	3000 (rpm)		6000 (rpm)		References
		COF	Wear rate (cm^3/MJ)	COF	Wear rate (cm^3/MJ)	
34	60	0.26	0.024	0.18	0.030	[34,35]
37	30	0.26	0.025	0.18	0.032	
38	80	0.28	0.025	0.18	0.035	
56	24	0.29	0.010	0.16	0.002	[37]
61	28	0.31	0.024	0.17	0.008	
45	19	0.28	0.003	0.15	0.002	
41	18	0.25	0.003	0.18	0.013	
53	19	0.25	0.010	0.16	0.002	[38]
58	20	0.26	0.040	0.16	0.004	
33	16	0.27	0.043	0.19	0.008	
50	14	0.31	0.010	0.21	0.008	
53	19	0.25	0.008	0.16	0.005	[39]
58	20	0.26	0.038	0.16	0.006	
33	16	0.28	0.042	0.20	0.010	
50	15	0.32	0.010	0.22	0.010	
23	18	0.36	0.018	0.26	0.024	[40]
23	24	0.34	0.015	0.24	0.025	
34	22	0.36	0.024	0.25	0.025	
32	28	0.34	0.042	0.26	0.024	
47	30	0.31	0.026	0.18	0.040	[45]
17	57	0.30	0.103	0.34	0.023	[50]
13	52	0.31	0.047	0.15	0.018	

complex. However, by identifying an optimal range of friction coefficients (0.29–0.34) and low wear rates (<0.18 cm^3/MJ), the hardness and thermal conductivity of CBFMs were found to fall within ideal ranges for achieving superior performance under different braking speeds: 20–30 HB for hardness and 55–70 W/m·K for thermal conductivity. The synergistic interaction between strength and thermal conductivity, along with their influence on braking performance, remains insufficiently understood. A larger dataset is essential to develop a comprehensive database correlating the mechanical, thermal, and braking properties of CBFMs, thereby offering a theoretical foundation for designing CBFM components that balance high friction coefficients with low wear rates.

3. Interfaces

The interfaces between components significantly affect mechanical and tribological properties of CBFMs, with interface characteristics serving as a key measure of the bonding state between matrix and components. In CBFMs, the interface mainly refers to micro-regions where significant changes of elements occur between the matrix and different components, forming interconnections capable of load transfer. The interfacial damage mechanisms critically influence the macroscopic braking performance of CBFMs.

3.1. Interface characteristics

The interface acts as a bridge facilitating the connection between matrix and components, with its characteristics serving as the basis for evaluating bonding property and optimizing composite design [66–69]. Based on the bonding state between the components and the Cu matrix, the interface types in CBFMs can primarily be categorized as follows (Fig. 5):

(I) Mechanical Bonding Interface. The bonding primarily relies on interlocking caused by the rough surfaces of the components and the contraction stress of the matrix. For example, some refractory metals and carbides, W and WC, and some ceramic abrasive components, the zirconia and silica, are characterized by high hardness and brittleness. In addition, owing to the inherent non-wettability and chemical inertness between copper and carbon. Graphite and carbon nanotubes (CNT) form mechanical bonds with copper [70,71]. During the formation of this interface type, no reaction or diffusion is observed. Instead, the increased surface complexity and roughness of the components expand the interfacial area, improving wettability between the components and the matrix and reinforcing the bonding at the original contact interface.

(II) Diffusion Bonding Interface. During the preparation of CBFMs, mutual dissolution and diffusion of elements occur between the reinforcement components and the Cu matrix, forming a diffusion layer of a specific thickness that characterizes this interface. Fe and Cu exhibit a certain degree of wettability, resulting in a well-bonded interface. Cu and Fe diffuse into the Fe and Cu matrices,

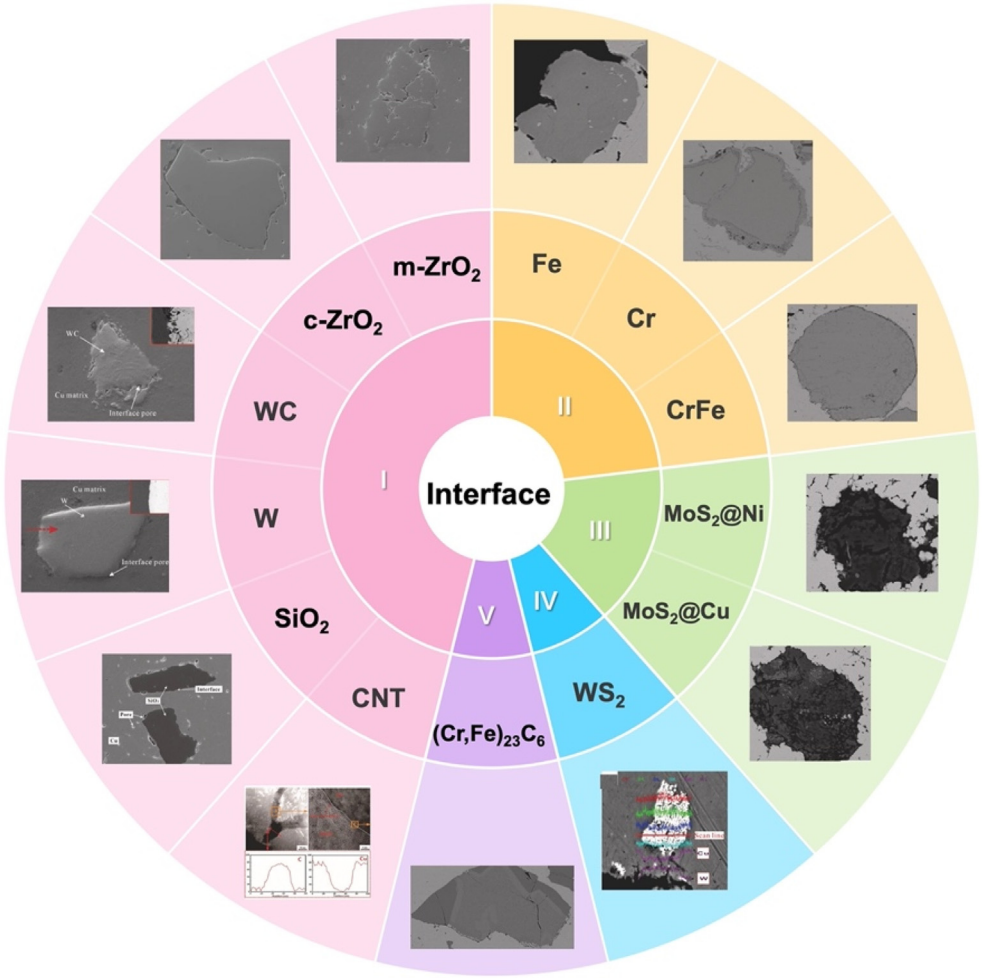

Fig. 5. Five typical interfaces of copper and components. I, II, III, IV, V correspond to mechanical bonding interface, diffusion bonding interface, coating bonding interface, reaction bonding interface, and mixed interface, respectively. Taken from Refs. [26–28,66,69,71] with permission.

respectively, forming Cu-enriched Fe-based substitutional solid solutions and Fe-enriched Cu-based solid solutions. The precipitation of Cu in the Fe matrix is relatively more pronounced than that of Fe in the Cu matrix. Mutual diffusion occurs between Cu and Cr, forming a diffusion layer with a thickness of 7 μm–10 μm. The diffusion layer at the CrFe/Cu interface is thinner and exhibits lower porosity compared to the Cr/Cu interface [26,27]. This type of interface commonly forms in metallic or alloyed reinforcement components with limited solubility in the copper. Impurity atoms in the matrix tend to deplete or concentrate at the interface, resulting in uneven dissolution and diffusion between the two phases, which often creates an irregular, interlocking dissolution-diffusion interface.

(III) Coating Bonding Interface. To enhance the interconnection between material components, certain reinforcement components are often coated with surface layers via electroplating or chemical plating, improving the bonding property between the reinforcement and the matrix. In this case, the interface between the reinforcement and matrix primarily consists of the interface formed by the coating and the matrix. For instance, as the MoS_2 coating transitions from Cu to Ni, Ni exhibits good retention of MoS_2 due to the absence of reactions between Ni and MoS_2 during sintering. The interface between MoS_2 and the Cu matrix transitions from a weak reaction bonding interface to a stronger coating bonding interface, with strength dependent on the diffusion layer formed between the coating and Cu matrix, resulting in higher strength than the reaction-bonded interface [55].

(IV) Reaction Bonding Interface. This type of interface refers to regions where chemical reactions occur between the reinforcement and matrix at the interface, producing new substances that bond with the matrix. Typically, chemical reactions and the resulting substances at the interface depend not only on the types of components but also on the fabrication process. A typical reaction interface involves the sintering reaction between copper and WS_2, resulting in the formation of copper sulfide and tungsten.

(V) Mixed Interface. Due to their complex characteristics, reinforcement components may form two or more aforementioned types of interfaces with the matrix. In such cases, the interface between the reinforcement and matrix is referred to as a Mixed Bonding Interface. For example, the eutectic phase $(Cr,Fe)_{23}C_6$ bonds with the Cu matrix through diffusion-mechanical mixing [28].

3.2. Micro and macro properties of components and matrices

By analyzing the sliding behavior at the interfaces between the Cu matrix and three types of abrasive components, including metals, alloys, and ceramics, as well as lubricating components, the overall sliding characteristics of each interface type can be obtained. As shown in Fig. 6, some metals and alloy abrasive components with high ductility, good toughness, and relatively low hardness, such as Fe, Cr, CrFe, and $(Cr,Fe)_{23}C_6$, tend to exhibit characteristics of deformation dominated by plasticity, high indentation depth, and a high COF during sliding [28].

In-depth analyses of the Cu/Fe interface under varying sliding pressures reveal that, despite significant plastic deformation, the bonding between Fe and Cu remains robust. The smaller hardness difference between Fe and Cu, combined with the high strength of their incoherent diffusion-bonded interface, promotes extensive plastic deformation without interfacial failure. In contrast, the Cr/Cu interface exhibits narrower scratch widths and reduced deformation due to the higher hardness of Cr abrasive components. However, at high load, localized interfacial delamination occurs at the Cr/Cu interface, marking the onset of partial damage. This limited plastic deformation along the sliding direction induces a steep rise in the COF, reflecting the damage progression at the interface [27]. Variations in CBFM braking curves are primarily governed by the properties of Fe and Cr as abrasive components and the wear surface differences associated with Fe/Cu and Cr/Cu interfaces. Diffusion-bonded Fe and Fe/Cu interfaces foster the development of mechanically mixed layers, granting Fe-containing CBFMs higher COF and better wear resistance compared to Cr-containing CBFMs, effectively curbing rapid wear escalation. Fe-containing CBFMs mainly exhibit delamination wear due to the failure of Cu/Fe composite layers. During the mid-braking phase, frictional heat accumulation causes pronounced Cu matrix softening in Cr-containing CBFMs, resulting in a sharper COF drop and a characteristic "saddle-shaped" braking curve. Cr-containing materials predominantly undergo delamination wear driven by matrix layer degradation.

As for mixed bonded layer of $(Cr,Fe)_{23}C_6$ compared with CrFe, which is diffusion bonded, the CrFe/Cu interface exhibits relatively high

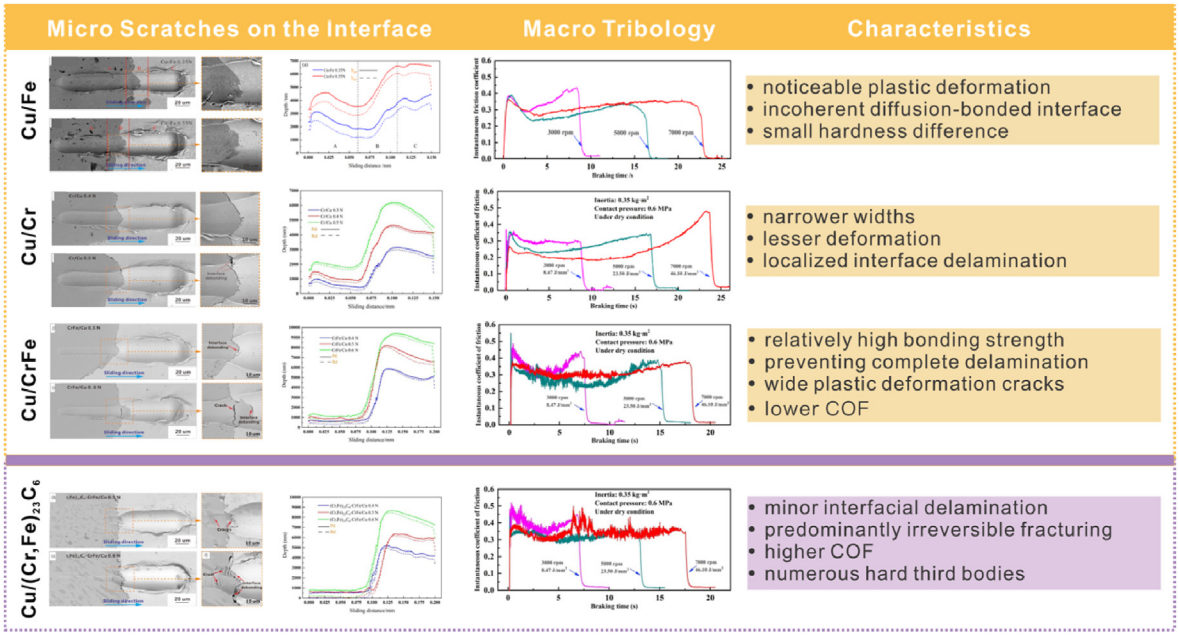

Fig. 6. Microscratches of Cu/Fe, Cu/Cr, Cu/CrFe, Cu/$(Cr,Fe)_{23}C_6$, and macro tribological properties of corresponding CBFM. Taken from Refs. [26,66] with permission.

bonding strength, preventing complete interfacial delamination. Under high pressure, in addition to localized delamination, wide plastic deformation cracks develop within the CrFe phase at the interface. Under high pressure, $(Cr,Fe)_{23}C_6$ phase particles at the interface begin to fracture, with minor interfacial delamination observed between this phase and the matrix. Deformation at the CrFe/Cu interface is primarily plastic, whereas deformation at the $(Cr,Fe)_{23}C_6$/Cu interface is predominantly irreversible fracturing [28]. In micro-scratch tests, the substantial average COF disparity between the two materials arises primarily from differences in indentation depth and deformation mechanisms. Localized interface failure results in an initial COF decline followed by a rapid increase. In alloy-based abrasive components, CrFe undergoes plastic deformation, yielding a higher COF, whereas $(Cr,Fe)_{23}C_6$ primarily undergoes elastic deformation, resulting in a lower COF. CBFMs with $(Cr,Fe)_{23}C_6$ predominantly exhibit delamination wear driven by the failure of plastic deformation layers, while CrFe-containing CBFMs mainly experience delamination wear due to degradation of the mechanically mixed layer.

As shown in Fig. 7, the bonding of Cu/W and Cu/WC interfaces, characterized by the absence of a reaction interface layer, is primarily mechanical. WC particles exhibit relatively loose and porous edges compared to W particles, influencing the interface's integrity under pressure. The debonding expands, reaching the edges of interface indentations, where cracks form within W particles, indicating the mismatch of Cu/W. In contrast, the Cu/WC interface remains intact under low pressures but undergoes significant spalling and WC particle fragmentation.

In terms of macro braking performance, CBFM with W forms a relatively intact and stable friction film during the sliding process. Work-hardening effects densify the surface, enhancing its hardness and stabilizing the friction process over time. Conversely, CBFMs with WC fail to develop a continuous friction film, as frequent material detachment and reintegration create a dynamic, renewing surface. Fragmented WC particles act as abrasive third bodies, intensifying surface wear and leading to prolonged fluctuations in the braking process. These contrasting behaviors highlight the critical influence of interfacial bonding strength, particle characteristics, and microstructural integrity on the overall braking performance of CBFMs.

Non-metallic abrasive components, such as ZrO_2, undergo localized fracturing under high sliding pressures. The m-ZrO_2 phase, with rougher surfaces and higher specific surface areas, forms stronger mechanical interlocks with the Cu matrix compared to c-ZrO_2, maintaining good bonding under all experimental pressures. In contrast, c-ZrO_2 interfaces delaminate at higher pressures, generating third bodies that destabilize the friction process. Macroscopically, m-ZrO_2's low fracture toughness causes delamination and instability in the COF, while c-ZrO_2, with higher fracture toughness, reducing COF fluctuations. However, weaker bonding makes c-ZrO_2 prone to delamination, creating peaks in friction curves [63–65]. The m-ZrO_2, with its lower hardness and surface undulations and fragmentation during sliding, exhibits an average friction coefficient three times higher than that of c-ZrO_2 components.

The interface failure of SiO_2, particularly at the edges of SiO_2 particles, is characterized by pronounced fragmentation and the formation of numerous brittle fracture cracks. Microscopically, a higher COF is exhibited by strongly bonded interfaces compared to weakly bonded Cu-SiO_2 interfaces. Macroscopically, during braking, the Cu/SiO_2 interface is transitioned from an initially weakly bonded mechanical interface to a simple mechanical bond formed between SiO_2 particles and the plastically deformed copper layer. Additionally, the failure mode of the Cu/SiO_2 interface is characterized by a transformation from mechanical bonding to the fracture of SiO_2 particles [23,31,33].

The high hardness of ceramic abrasive components primarily results in elastic deformation during sliding, leading to lower friction coefficients. Despite their superior overall hardness, ceramic abrasive components form weak mechanical bonding interfaces with the matrix. During friction, these components are prone to delamination or fragmentation, losing their reinforcing effect. Consequently, CBFMs containing ceramic abrasive components exhibit the largest reduction in COF. Alloy abrasive components combine the advantages of both metallic and ceramic abrasive components, forming diffusion or mixed

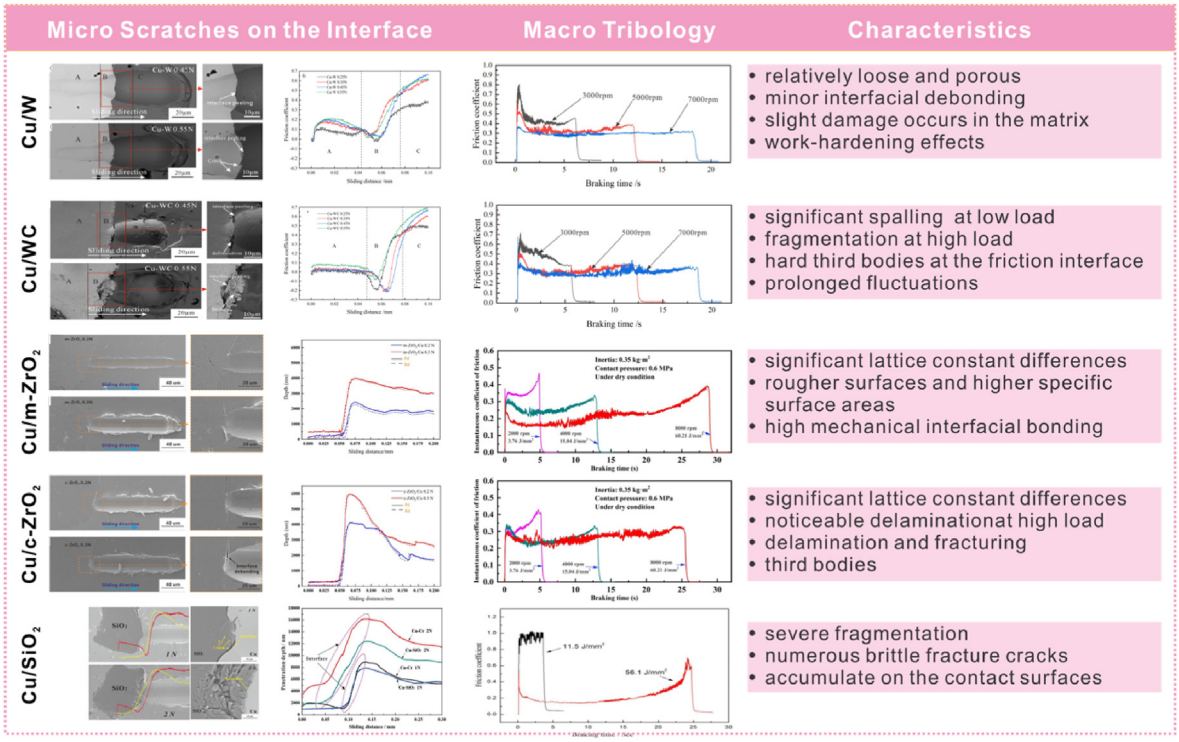

Fig. 7. Microscratches of Cu/W, Cu/WC, Cu/m-ZrO_2, Cu/c-ZrO_2, Cu/SiO_2, and macro tribological properties of corresponding CBFMs. Taken from Refs. [26,69] with permission.

bonding interfaces with the matrix. These components achieve a balance of relatively high hardness and adequate interfacial bonding strength, resulting in superior friction-enhancing performance. Among them, $(Cr,Fe)_{23}C_6$ exhibits the best friction enhancement due to its high hardness and its ability to absorb braking energy through fragmentation.

The interfaces of graphite primarily exhibit mechanical bonding characteristics. Fine natural graphite, due to its higher degree of graphitization, demonstrates superior lubricity. In contrast, granular graphite possesses higher strength, but its interaction with copper induces more pronounced microstructural changes. Fine natural graphite can be uniformly distributed within the copper matrix. On a microscopic scale, the tribological performance is governed by the material's plowing and adhesion forces. The friction coefficient associated with the plowing force increases with the applied normal load and exhibits a marginal upward trend as the graphite content increases. As depicted in Fig. 8a, at low graphite content (below 6 vol%), the surface layer experiences sustained shear stress, initiating microcrack propagation in the subsurface, which subsequently culminates in surface tearing. When the graphite content is sufficient (ranging from 6 % to 20 vol%), a lubricating film is formed on the surface. This graphite-based lubricating film effectively mitigates direct contact between the indenter and the composite material. At graphite contents exceeding 20 vol%, cracks and dislodged graphite particles are evident (Fig. 8c), attributed to the weak interfacial bonding between the copper matrix and graphite particles [70]. Fig. 8e and f illustrate the crystal structure of copper surrounding graphite particles and the corresponding nanoindentation results. Owing to disparities in strength and wettability, the crystal size of copper in proximity to graphite particles within CBFM is markedly reduced, accompanied by a substantial accumulation of dislocations. Consequently, the hardness and elastic modulus near the interface exhibit a significant reduction [12]. When frictional forces traverse this region, the pronounced deformation of copper results in the accumulation of defects, a rapid escalation in surface energy, and a heightened likelihood of severe wear. Therefore, enhanced solutions are required for the copper-graphite interface, such as surface coating treatments applied to graphite particles.

The other lubricating components represented by CNT and MoS_2 exhibit excellent lubricating properties due to their layered structures. This structure allows them to maintain a low COF during sliding, even at higher indentation depths (Fig. 9). The COF trend remains positively correlated with applied pressure. The enhancement of mechanical properties through the incorporation of CNTs significantly reduces the wear track depth observed during testing. With increasing CNT content, the direct contact area with the counterpart decreases during friction testing. As a result, the likelihood of adhesive wear is reduced. Moreover, the addition of CNTs potentially imparts the CBFM with lubricating properties [71]. Changes in WS_2 volume content alter the actual contact surface during scratching, transitioning from predominantly Cu-based contact to increased WS_2 contact, thereby reducing the COF. Under shear forces, WS_2 spreads along the friction surface, enhancing its lubricating effect. Therefore, the macro tribology can be interpreted as a repetitive stacking of micro-scale scratching events. The Ni coating slows the reaction rate between Cu and MoS_2, the interface formed between MoS_2@Cu and the Cu matrix is a relatively intact diffusion-reaction bonded interface. However, some MoS_2 still undergoes a chemical

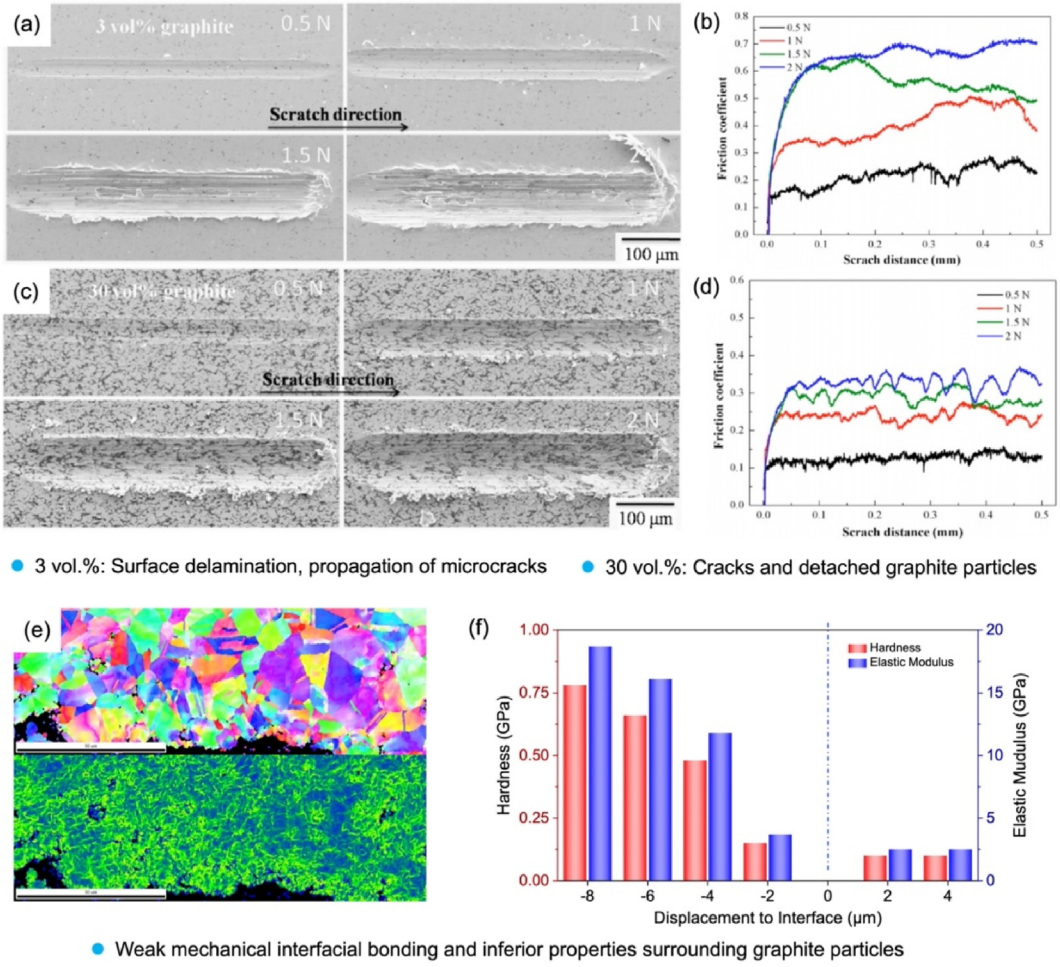

Fig. 8. Microscratches and tribological properties of Cu/Graphite interfaces. (a, b) Cu with 3 vol% natural graphite; (c, d) Cu with 30 vol% natural graphite; (e, f) Cu and Graphite particles. Taken from Refs. [12,70] with permission.

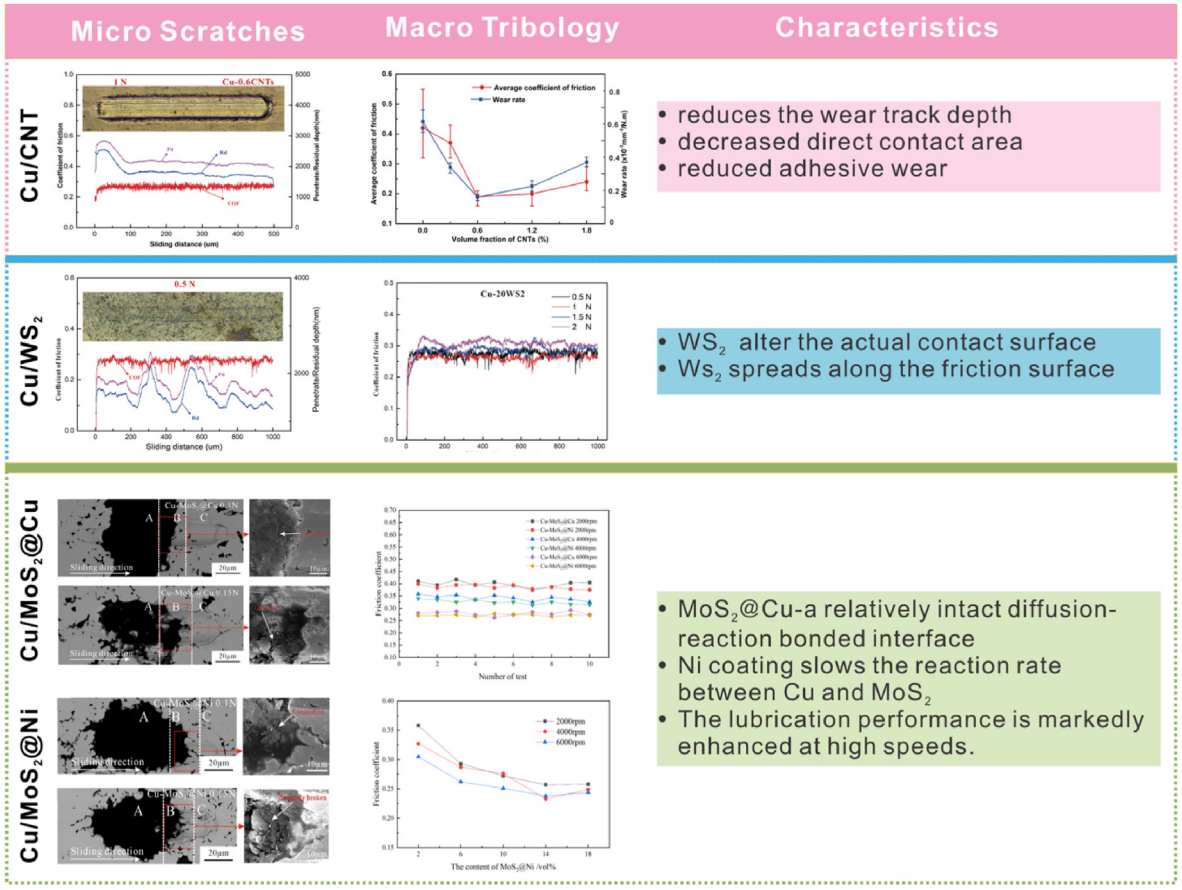

Fig. 9. Microscratches of Cu/CNT, Cu/WS_2, Cu/MoS_2@Cu, and Cu/MoS_2@Ni interfaces; and macro tribological properties of the corresponding CBFM. Taken from Ref. [71] with permission.

reaction with Cu, resulting in a diffusion-reaction bonded interface. Under low-speed conditions, the absence of a complete MoS_2-containing oxide film on the surface results in numerous furrows and adhesive pits on the friction surface. In this stage, the primary wear mechanisms are a combination of adhesive wear and plowing wear. As speed increases, a lubricating oxide film gradually forms on the material surface, with wear debris coating the surface. While the oxide film's thickness increases, its internal bonding strength decreases. At this point, the wear mechanisms for both materials gradually shift to fatigue delamination wear of the oxide film.

With the transition of abrasive components from metallic to non-metallic and the gradual decrease in interface strength, the post-sliding state of the interface progressively changes. It shifts from deformation along the sliding direction in Fe/Cu diffusion-bonded interfaces to slight deformation and localized delamination in CrFe/Cu and Cr/Cu diffusion-bonded interfaces. This transition continues toward localized delamination and hard phase fracturing in $(Cr,Fe)_{23}C_6$-CrFe/Cu mixed-bonding interfaces, followed by delamination in the coating interfaces of MoS_2@Cu/Cu and MoS_2@Ni/Cu, and ultimately extensive delamination in c-ZrO_2/Cu mechanical bonding interfaces, or even to extensive delamination and hard phase fracturing in SiO_2/Cu mechanical bonding interfaces.

In diffusion-bonded interfaces, the high interfacial strength and resistance to complete failure provide support for the indenter, helping to slow the rapid increase in indentation depth and COF. Additionally, after sliding at low pressure, partial elastic recovery may occur in the interface, resulting in relatively low deformation parameters. Although coating-bonded interfaces are weaker than diffusion-bonded interfaces, they still provide some degree of support. This results in a relatively smooth transition of the COF at the coating interface. Under higher sliding pressures, the brittle hard phases within the interface are highly likely to fracture. Both crystalline forms of ZrO_2 form mechanical bonding interfaces with the Cu matrix, where the interfacial strength depends on the degree of mechanical interlocking. This results in the lowest interfacial bonding strength.

Overall, the interfacial property between components and the matrix is a crucial factor influencing the intrinsic tribological characteristics. Suitable reinforcement components must not only exhibit strong interfacial property with the matrix but also possess favorable intrinsic tribological characteristics. Considering both interfacial property and the intrinsic characteristics of reinforcement components, along with the elemental control requirements specified in high-speed train braking friction material standards, the most frequently used reinforcement components in designs of CBFMs include Fe, ZrO_2, and CrFe.

4. Tribo-layers

The surface layer of friction pair materials undergoes significant changes in microstructure, composition, and morphology due to the cyclic interplay of shear stress, compressive stress, thermal accumulation, and environmental factors. This process leads to the formation of a distinct material zone, known as the tribo-layer, which exhibits markedly different properties and composition from the substrate. The tribo-layer structure primarily consists of a dual-layer system: a deformation layer and a friction film, both gradually derived from the substrate under frictional forces [72]. Regarding the deformation layer, studies by Rainforth and Rigney suggested that this layer originates from the plastic flow of surface materials induced by frictional shear stress [73,74]. During this plastic flow, grains are forced to elongate and fracture, while grain boundaries rotate toward the direction of shear stress, resulting in

reorientation and progressive refinement of the microstructure within the deformation layer. Both material properties and operating conditions influence the morphology and structure of the deformation layer. For example, increasing material plasticity, reducing hardness, and raising frictional load and relative sliding speed effectively increase the thickness of the deformation layer. Conversely, enhancing stacking fault energy and lowering the temperature at the frictional interface can promote grain refinement within this layer.

4.1. Micro tribo-layers

Plastic deformation induced by friction within the subsurface confined layer facilitates the dissipation of frictional energy [75–77]. For example, the COF in face-centered cubic (FCC) metals, such as copper, is minimized when sliding occurs along close-packed (111) planes [78]. Friction-induced plastic deformation differs from work hardening in that it results in surface hardening and oxidation.

Due to the presence of substantial metal and non-metal phases in CBFMs, the theoretical studies on crystal tribology and origin of deformation layer remain primarily focused on the deformation of pure copper [79]. Normal slip and grain boundary sliding under frictional loading differ from monotonic deformation modes such as indentation and tension in nanocrystalline materials. When the grain size is reduced to tens of nanometers, deformation is no longer dominated by normal slip but is instead controlled by partial dislocation activity [80,81]. Free surfaces can serve as effective sources of dislocations [82]. Large shear strains and steep strain gradients near the surface induce a high density of geometrically necessary dislocations (GNDs). Under extremely low sliding speeds (0.5 mm/s), dislocation trace lines are generated in the subsurface of coarse-grained (~50 μm) pure copper at the onset of sliding [83,84]. Greiner investigated the early-stage deformation mechanisms within the shear-affected zone under copper sliding contact. At the twin boundary beneath the sliding interface, two pronounced horizontal dislocation trace lines (DTL) were identified, serving as indicators of the active deformation mechanism. Additionally, subsurface regions exhibited localized shear along the primary DTL in the sliding direction, accompanied by crystal rotation parallel to the transverse direction (Fig. 10a–c) [85]. The subsurface structural evolution of copper and its dominant deformation mechanisms were investigated through cyclic sliding experiments using sapphire spheres. Kikuchi diffraction, compared to EBSD, provides superior crystal orientation data during the transmission process of metallic friction deformation, especially for GNDs. TEM analysis confirmed the formation of subsurface DTL in copper during the reciprocating phase of the friction pair, which subsequently led to the emergence of nano-twins (Fig. 10d–i) [86]. Crystal orientation analysis reveals a strong compatibility with the theoretical models of these frictional deformation mechanisms. Quantitative separation of these distinct deformation mechanisms is critical for future predictive modeling of tribological contacts.

FIB-TEM is widely used for qualitative analysis of CBFMs, specifically for examining surface oxide layers several microns thick (Fig. 11a–e) [37,87]. As shown in Fig. 11f and g, the uppermost layer consists of a nano-oxide layer enriched with ceramic components, which resides a mechanically mixed layer of iron and copper beneath. This mixed layer is generated through secondary sintering following matrix deformation, fracturing, and subsequent oxidation. The uppermost layer of CBFMs with TiC-B_4C comprises fine nanoparticles (C, Cu, Fe, B, O, and Ti), generated through repeated compression of debris from the worn surface. The intermediate layer consists of graphite and B_2O_3, while the bottom layer corresponds to the matrix deformation region. Localized

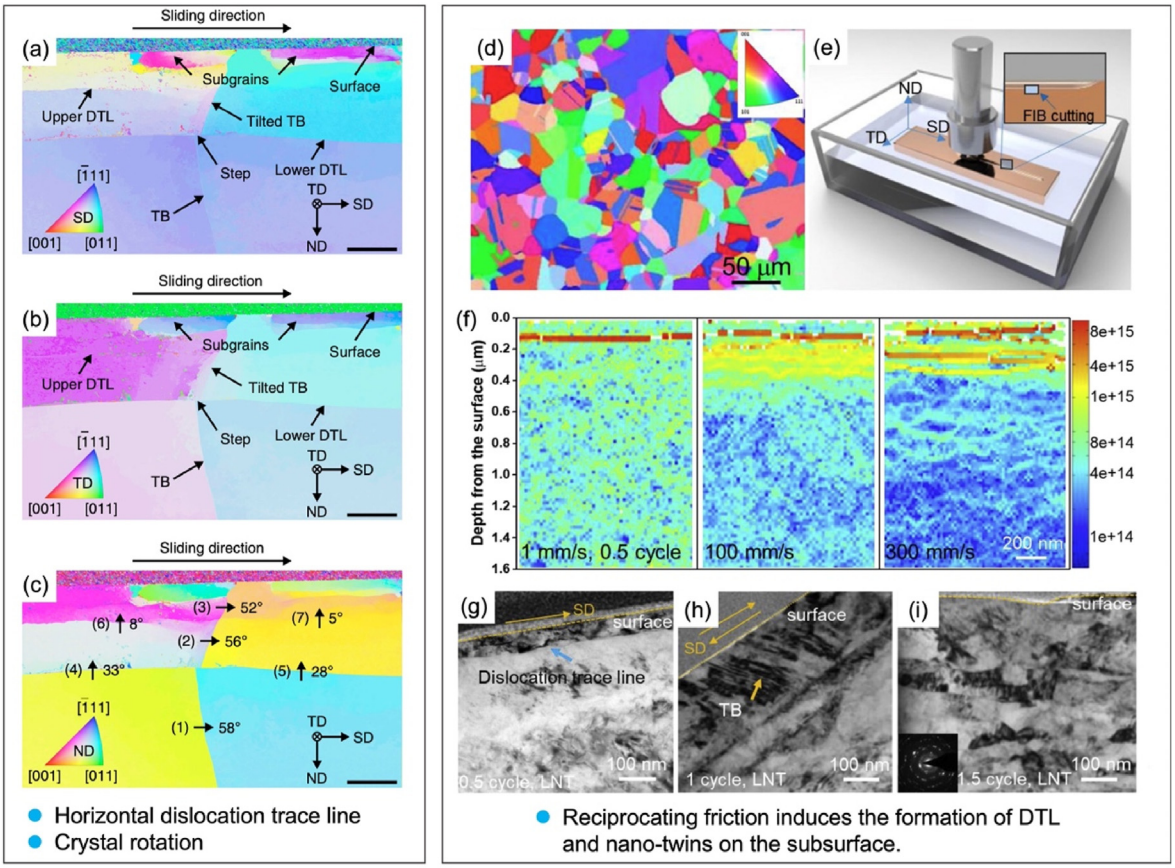

Fig. 10. The friction-induced deformation mechanisms of pure copper. (a,b,c) Crystallographic orientation data of tribologically deformed microstructure after a single sliding pass; (d,e) EBSD of pure copper and test methods; (f) analysis of the GND within the cross-sectional area of the copper sample; TEM bright-field images of copper samples subjected to low-temperature sliding at varying sliding cycles: (g) 0.5 cycle; (h) 1 cycle; (i) 1.5 cycles [85,86].

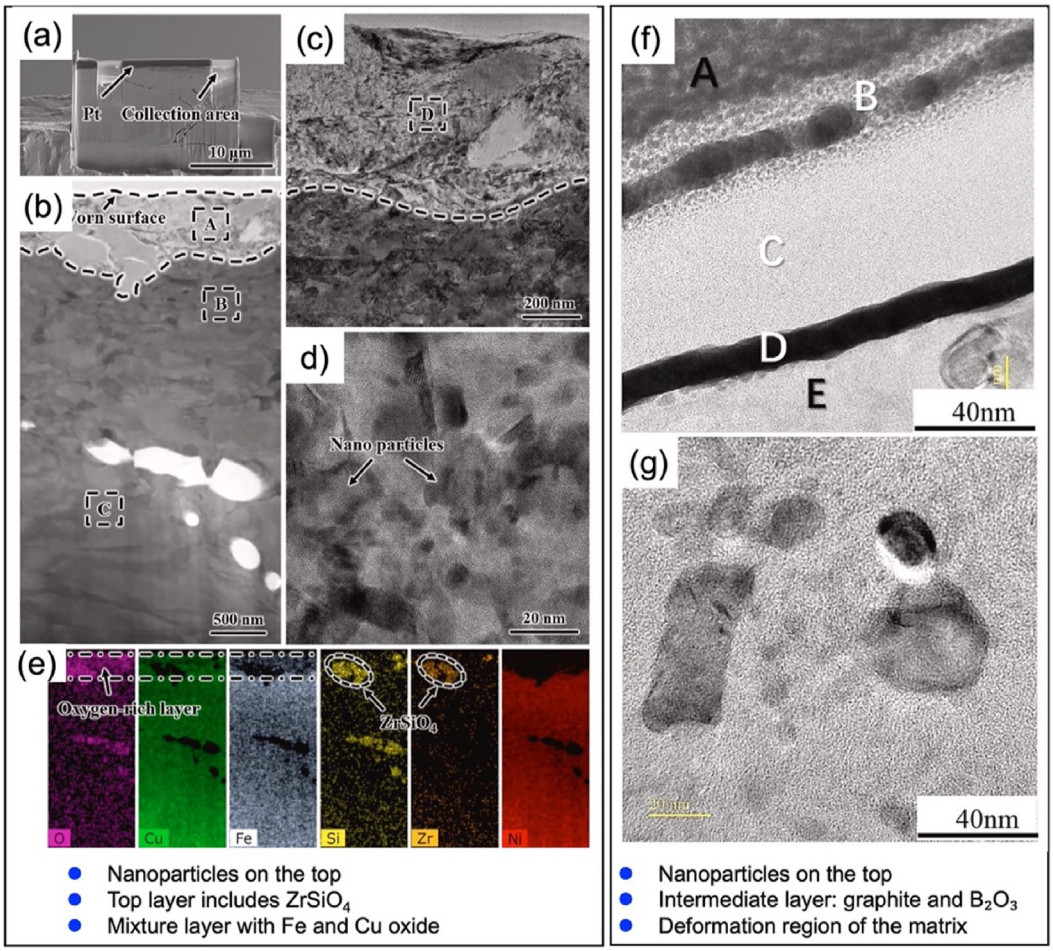

Fig. 11. FIB-TEM of tribo-layers in CBFM. (a–e) CBFM at braking energy density of 120 J/mm^2 for 20 cycles. (f,g) Differentiation tribo-layers of CBFM with TiC-B_4C. Taken from Refs. [37,87] with permission.

analysis poses significance in capturing the complete evolution of the tribo-layer, but qualitative analysis alone is insufficient for advancing the development of new CBFMs. During high-energy braking, the friction film actively participates in the friction process, exhibiting a more complex structural evolution compared to the plastic deformation layer. Under varying friction pair material systems and operating conditions, the friction film may develop distinct morphological and property characteristics.

4.2. Macro tribo-layers

The macroscopic characteristics of the tribo-layer provide a more accurate representation of the wear mechanisms compared to the characterization of the ultra-thin surface oxide layer, Fig. 12a shows the three typical tribo-layer structures of CBFMs: mechanical mixture layer (MML), plastic deformation layer (PDL), and cracks [88]. As shown in Fig. 12b and c, the first layer, referred to as the debris layer, consists of detached microscopic wear debris particles. This results from wear debris on the CBFM surface being severed by plowing forces in the later friction stages. The second layer is an MML, composed of deformed copper and iron formed through the secondary sintering of wear debris. The third layer is an oxidation layer formed by the deformation and oxidation of iron particles following copper delamination. The final layer consists of deformed iron.

The regulation of the tribo-layer is intrinsically linked to energy absorption, with the modulation of MML and its impact on PDL governed by the regulatory capacities of the components. With the addition of functional components such as Cu@GO, a uniform MML predominantly forms. By comparing the nanoindentation properties of the layered tribo-layers with those of the original matrix, it is revealed that graphene contributes to the absorption of large brake energy, rather than excessive wear caused by intense metal deformation and oxidation [15]. Hence, the MML exhibits an essential role in the tribological properties. As reported in previous research, the MML prevents direct contact between the substrate and the counterpart material, effectively reducing the wear rate [89]. Further oxidation of the MML and the propagation of fatigue cracks facilitate its delamination, resulting in the accumulation of particle-like lamellar wear debris. The formation and fragmentation of abrasive particles are two competing processes. Once fractured, the resulting fine abrasive particles agglomerate to form new abrasives [90]. In such cases, the primary wear mechanism is mechanical mixing, which is a subset of tribo-chemical reactions [91]. Under these conditions, oxidation of the MML may also lead to minor oxidative wear.

4.3. Wear mechanism

Discussions on wear mechanisms are predominantly based on the characteristics of the tribo-layer and wear debris damage. The microstructural characteristics of tribo-layers serve as indicators of underlying wear mechanisms, leading prior research to concentrate largely on qualitative analyses of these layers. Research indicates that at braking speeds below 200 km/h, abrasive wear predominates, maintaining a relatively low wear rate. The tribo-layer, comprising an oxide film, nanocrystalline, and deformed layer, contributes significantly to the

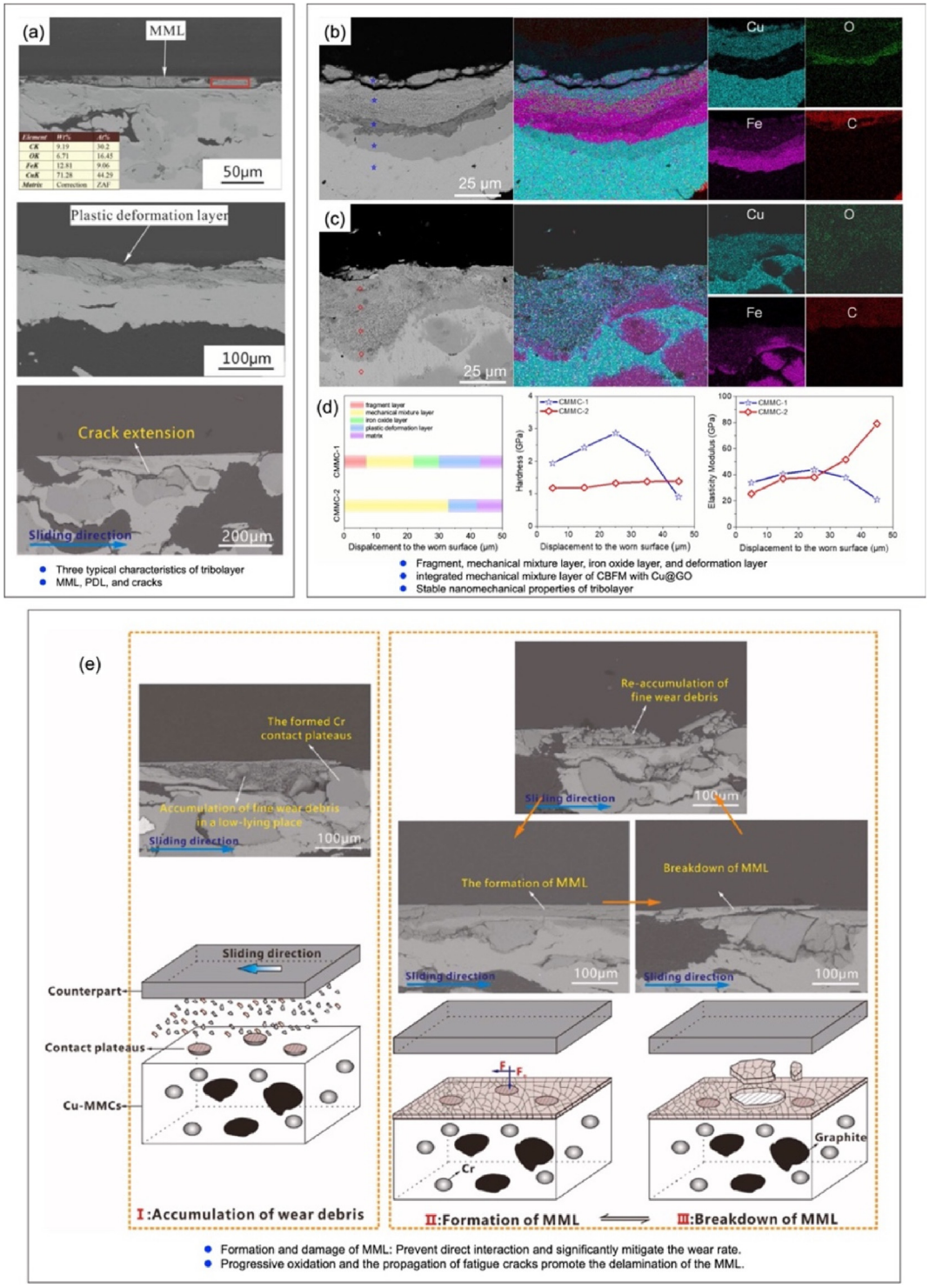

Fig. 12. Different formations of tribo-lyers in CBFMs. (a) MML, PDL, and cracks; (b–d) CBFMs without and with Cu@GO, and nanoindentation; (e) formation and damage of MML. Taken from Refs. [15,27,88] with permission.

enhancement of material friction and wear resistance [92,93]. Between 250 and 320 km/h, oxidative wear becomes the primary wear mechanism [94]. Xiao et al. identified a nanostructured oxide layer, primarily composed of CuO and Fe_2O_3, on the surface of commercial CBFMs subjected to braking at 380 km/h [95]. Moreover, CBFM exhibits peeling and pronounced oxidative wear, resulting in a relatively high wear rate (Fig. 13a). As braking cycles increase, the tribo-layer within CBFM experiences substantial alterations in both its properties and thickness.

Furthermore, the wear mechanisms of CBFMs, reinforced by various components, are inferred from the progressive evolution of the tribo-layer. As shown in Fig. 13b, Chen compares the wear mechanisms of CBFMs under 120 J/mm^2. Wear debris forms a dense tribo-layer due to weak adhesion between the counterparts and CBFMs. This tribo-layer, with high hardness and oxidation resistance, ensures low wear rates, high COF, and stable braking [87]. As for two new typical lubricant and abrasive components, like pitch coke and TiC-B_4C [37,50], Pitch coke reduces metal damage, as shown by decreased wear volume and improved debris morphology. An oxidized deformed metal layer and

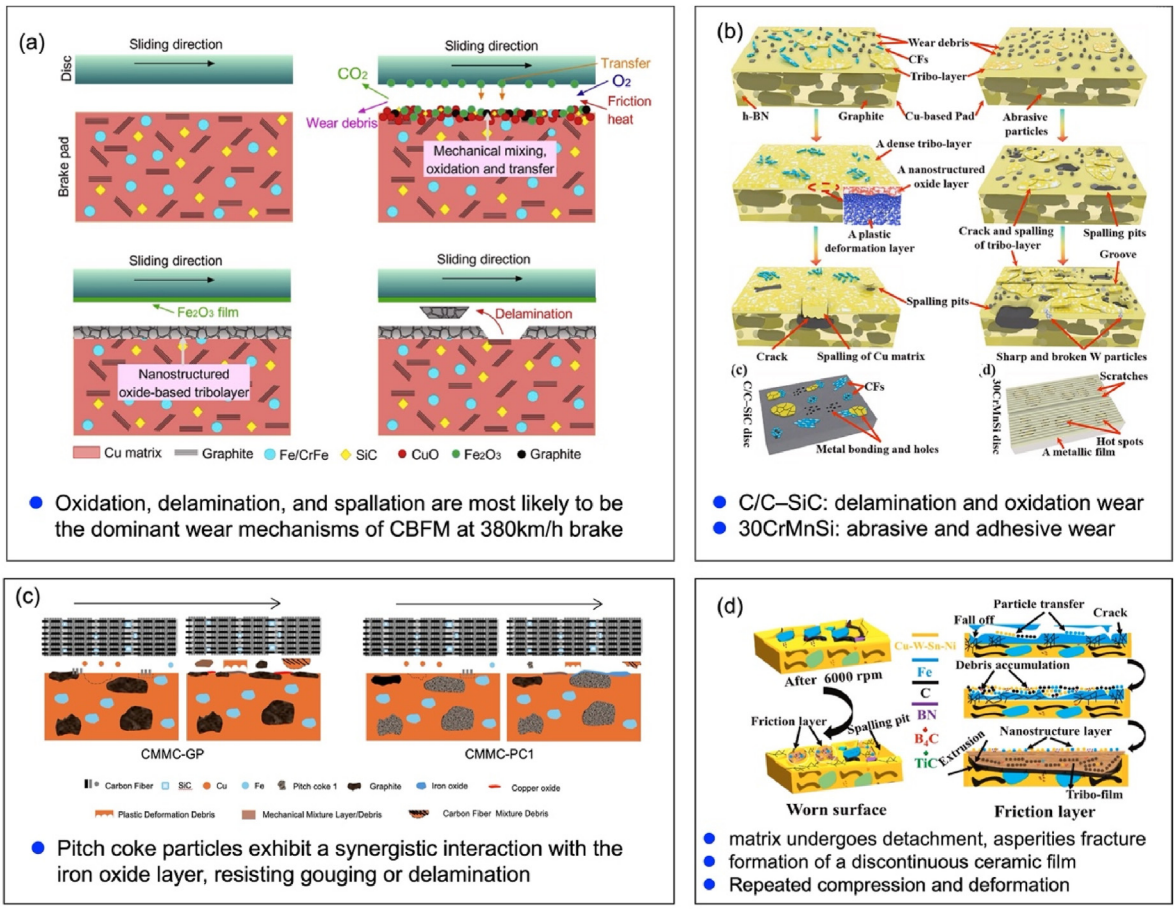

Fig. 13. Schematic diagram illustrating the wear mechanism of CBFMs. (a) CBFM at 380 km/h braking speed. (b) CBFM at braking energy density of 120 J/mm^2 (c) CBFM without and with pitch coke. (d) CBFM with TiC-B_4C. Taken from Refs. [37.50,87,95] with permission.

pitch coke exhibit excellent synergistic effects (Fig. 13c). In addition, the tribo-layer on TiC-B_4C worn surface forms primarily near Fe. Early braking detaches the soft matrix (Cu, Fe) and breaks ceramic particles, filling peeling pits. Oxidized particles create a discontinuous film, later forming a tribo-film mixed with graphite. This high-hardness layer prevents oxidation, ensuring low wear and stability (Fig. 13d).

Generally, wear originates not only from the surface but also from the subsurface of materials. Surface wear is directly caused by material removal through micro-cutting processes. Subsurface wear is closely associated with subsurface peeling, caused by material accumulation [96]. Consequently, wear rate is influenced not only by hardness but also by the elastic and plastic properties of the tribo-layer. It is widely acknowledged that low wear rates primarily occur at interfaces with weak interactions, in contrast to those with strong interactions, such as metallic bonds [97]. As a multi-component composite material rather than a single alloy, CBFM not only undergoes metallic plastic deformation under braking conditions (although the latter predominates) but is also significantly affected by the MML formed via secondary sintering of fine wear debris during severe deformation, along with the contribution of partially exposed non-metallic components, such as graphite particles. These factors further challenge the uniformity of the microscopic composition and mechanical strength of the tribo-layers. Developing CBFMs suitable for high-speed trains with higher speed necessitates a comprehensive elucidation of wear mechanism evolution within the complex tribo-layer structure, encompassing oxidation, plastic flow, sub-surface matrix transfer, and wear debris accumulation throughout sustained braking cycles. The accumulation of wear debris represents not only the degradation of CBFM itself but also encompasses damage to the tribo-layers under cyclic braking conditions. Consequently, the energy dissipated through wear within the tribo-layers and wear debris constitutes a critical yet understudied factor influencing braking properties.

Consummating a theoretical foundation contributes to supporting the development and implementation of CBFMs for high-speed trains at elevated operational velocities. A theory was developed to elucidate the formation and damage of the tribo-layers in CBFMs under high-energy braking conditions, offering novel perspectives on wear mechanisms [98]. As illustrated in Fig. 14a, the classical energy wear theory posits that the elastic energy stored per unit volume of wear debris is proportional to the deformation energy of metallic wear, contingent on the ratio of material hardness to the square of its elastic modulus. During friction, the energy associated with wear debris is equivalent to the surface energy; however, when wear occurs, the total energy of wear debris (E_{es}) surpasses the surface energy of the friction interface (E_A).

Under extreme high-energy braking conditions, CBFMs experience significant volumetric wear, rendering surface energy alone insufficient to accurately describe the formation and damage of the tribo-layers. Building upon the energy relationship between worn surfaces and wear debris as described in classical energy wear theory, and integrating the thickness of sub-surface and wear debris tribo-layer under high braking energy conditions, an innovative ratio t is introduced to characterize the dynamics of tribo-layers formation and damage. As depicted in Fig. 14b, a novel linear parameter (A') is proposed to investigate the surface area characteristics of sub-surface and wear debris tribo-layers. The cohesive energy is employed to quantify the deformation energy of the sub-surface tribo-layer in CBFM, wherein this deformation energy (E_D) is lower than that of E_{es}. By establishing the relationship between these two energies, the sub-surface's tribo-layer thickness (D) and the wear debris's tribo-layer thickness (d) are associated with the formation and damage of

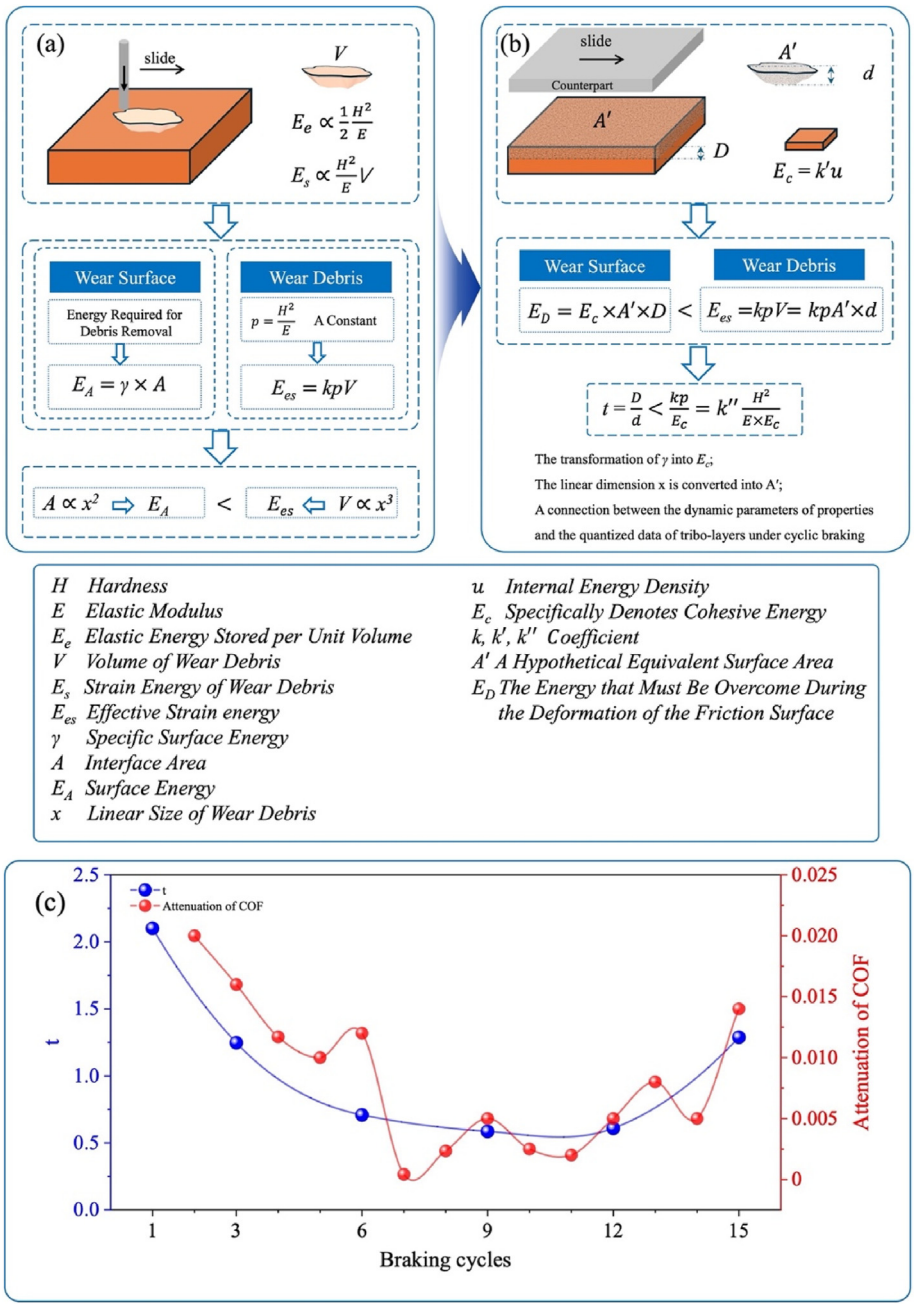

Fig. 14. New theory based on quantitative evolution of tribo-layer of CBFM. (a) Classical energy wear theory. (b) New theory of formation and damage of tribo-layer, (c) Correspondence of ratio *t* and COF. Taken from Ref. [98] with permission.

tribo-layer, respectively. The ratio *t* is defined to quantify the relationship between these thicknesses and is correlated with the dynamic mechanical properties (hardness and elastic modulus) of tribo-layers.

Utilizing the defined tribo-layer formation and damage ratio *t*, the variations in *D* and *d* with braking cycles in CBFM were quantitatively characterized, providing insights into the relationship between changes in *t* and tribological performance (Fig. 14c). The variation of *t* demonstrates a strong correlation with the magnitude of COF decay. By integrating the relationship among *t*, the mechanical properties, and the structural characteristics of the tribo-layer, the wear mechanism was elucidated.

Within this theory, the performance and structural characteristics of the tribo-layers are correlated with their tribological behavior. This novel energy wear theory warrants further development, including hardness and elastic modulus testing, as well as energy simulation calculations. Although the correlation between the decline in the COF and *t* substantiates the role of tribo-layers, the wear rate variation pattern has yet to be accurately aligned with the predictions of the energy wear theory. This holds significant implications for advancing the lifetime prediction of CBFM based on tribo-layer characteristics.

5. Challenges and limitations

5.1. Challenges

Braking property is not an intrinsic property of CBFM but rather a system attribute closely associated with the external service environment under specific application conditions [99]. For instance, during emergency braking in high-speed trains, CBFM operates under high-speed, intense thermal braking conditions, often encountering extreme

climate environments, putting them in an extreme braking state. The extreme braking conditions and adverse climates can cause abnormal wear on CBFM. More demanding service environments impose stricter requirements on the stability of CBFM under wide temperature ranges and high load conditions.

5.1.1. High energy and high temperature

Researchers have converted harsh braking energy into energy wear, based on the theory that energy dissipation during friction causes wear; fundamentally, wear behavior is a process of energy transformation and dissipation [100]. Based on this principle of energy transfer and wear, and considering the evolution of thermal, mechanical, and tribological properties at the material's surface interface under braking pressure, the braking process can be summarized as the transformation and dissipation of kinetic and thermal energy in a thermo-mechanical coupling system. Desplanques et al. dimensionally analyzed braking speed, time, and other parameters as input values and found that, under different input conditions, consistent trends in average surface temperature and temperature field evolution could be observed, along with similar braking property trends [101]. This confirmed the correlation between kinetic and thermal energy and introduced a temperature-based experimental method for brake pad surface evaluation, offering valuable insights for studying brake pad properties under harsh conditions. Peng et al. replicated the emergency braking process at speeds up to 380 km/h, using the aforementioned equivalence criteria. As braking speed increased, brake pad wear consistently rose, COF decreased, and tailing was not prominent, while exposed or pitted regions, even ablation holes, appeared on the worn surface [94]. Xiao et al. considering thermal energy as a substitute for kinetic energy, heated CBFMs to 800 °C before performing braking tests [102]. The high thermal energy oxidized surface elements to higher valence states, causing wear debris and oxides to adhere more readily to the softened copper matrix, forming a mechanically mixed layer that hindered direct contact with the counter material, thus reducing wear.

Based on the braking behavior of CBFMs under thermo-mechanical coupling, and with comprehensive consideration of geometric and energy factors, researchers have begun using energy density as an equivalent measure to evaluate CBFM property under more demanding conditions. Firstly, using energy density as a primary reference factor, constructing a scaled-down equivalent experimental platform, showed good agreement with the results from bench tests [103]. Zhou et al. classified braking energy density into three levels: low (<10 J mm^{-2}), medium (10–30 J mm^{-2}), and high (>30 J mm^{-2}) [27]. They developed a friction and wear mechanism map correlating braking energy density with the composition of CBFM, providing a reference for designing materials suitable for higher-speed applications. Xiao et al. found that with increasing braking energy density, the braking stability of CBFM decreases, and the wear rate shows a clear upward trend. At high energy densities, wear mechanisms are predominantly characterized by delamination wear, abrasive wear, and oxidative wear [104].

Currently, for 400 km/h high-speed trains under emergency braking, CBFMs are required to dissipate braking energy approximately 78 % higher than that of 300 km/h, a demand that surpasses previously reported studies and represents a particularly extreme service condition (Fig. 15a). The average temperature reaches 600–700 °C, with flash temperatures peaking at 900 °C. Under such high-temperature conditions, rapid oxidation and mass loss occur in the CBFM (Fig. 15d and e) [4]. However, the microstructural evolution of the constituent phases and the formation and damage mechanisms of the tribo-layer under these extreme energy-dissipating conditions remain unclear [105]. Although research in this area is relatively limited, it remains highly significant. By integrating energy transfer and dissipation under actual service conditions, and considering factors such as energy density and temperature

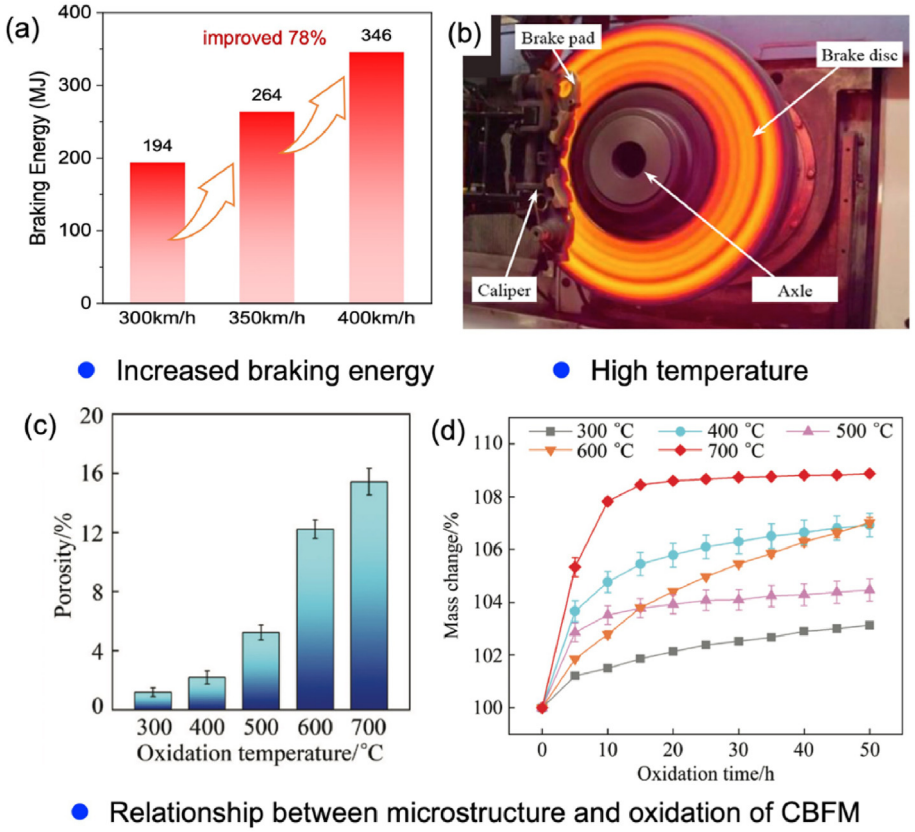

Fig. 15. Effect of high energy and temperature on CBFM. (a) Braking energy at different emergency braking speeds. (b) Emergency braking of high-speed train brake. (c) Porosity of CBFM oxidized at different temperatures. (d) Isothermal oxidation curves of Cu-based brake pad at temperatures from 300 to 700 °C. Taken from Refs. [4,6] with permission.

field distribution, a comprehensive property evaluation method for CBFM can be developed. This approach will elucidate the evolution mechanisms of material components and tribo-layers in response to energy formation and dissipation, providing a theoretical basis for the development of novel CBFMs.

5.1.2. Climatic environment

In designs and development of CBFMs for special operating conditions, it is essential to consider the harsh climatic environments encountered by high-speed trains, such as extreme cold and large temperature variations. These factors can directly alter the contact state between brake pad materials and the brake disc, thereby affecting braking property and wear mechanisms. Ma et al. investigated the braking behavior of CBFMs at ambient and sub-zero temperatures (−30 to 20 °C) and found that as temperature decreases, the wear rate would initially increase and then decrease, with wear patterns shifting from adhesive wear to large-scale spalling [106]. Under extreme cold conditions, the cold welding effect of hard ice and snow particles can easily form a frozen encapsulation layer on the brake pad surface, leading to mechanical braking failure [107]. In rainy and snowy conditions, snowflakes and rain can form an icy tribo-layer on the brake pad surface, reducing the COF [108]. Meanwhile, flowing water reduces the tendency for wear debris to accumulate, inhibiting tribo-layer formation, although the resulting water film substitutes for the tribo-layer's function. Increased humidity can reduce the equilibrium temperature of the brake pad surface, alleviating spalling and abrasion effects on the material, which in turn decreases the COF and wear rate [109]. CBFM tends to absorb moisture in humid atmospheres, which is stored in micro-pores on the surfaces. Under high braking temperatures, this moisture rapidly vaporizes. Due to the close contact between CBFM and their counterparts under high braking pressures, these vapor bubbles struggle to escape from the contact interface [110]. During high-speed friction, they are prone to rupture, generating intense impact pressures that accelerate material damage and lead to cavitation. Therefore, the cavitation issues caused by moisture in high-speed braking systems warrant serious attention, and extensive theoretical research is still needed in this area [111].

5.2. Limitations

5.2.1. Synergy of multi-component and interfaces

With the continuous increase in high-speed train operating velocities, CBFMs face challenges such as insufficient braking capacity, braking instability, and high-temperature thermal degradation, significantly impacting service property. Consequently, designing high-property CBFMs that can withstand harsh service conditions has become a critical focus. In the increasingly demanding braking environment, achieving a high volume fraction of lubricant- and abrasive-regulating components on the friction surface is fundamental to ensuring superior braking properties in CBFMs. Furthermore, the increased braking interface temperatures necessitate a higher volume of components with properties such as heat resistance, energy absorption and thermal degradation resistance, leading to a marked "ceramic-like" design tendency in high-property CBFM. However, it is noteworthy that while a ceramic-like design improves the tribological property of friction materials under extreme high-energy conditions, it also significantly increases internal defects and rapidly deteriorates fundamental physical properties such as overall strength, hardness, and toughness, making the material susceptible to abnormal failure under extreme braking conditions. Therefore, ceramic-like design in CBFMs must also consider the material's overall need for enhanced strength and toughness. It can be concluded that designing high-property CBFM results from a balanced coordination and mutual compromise between ceramic-like and toughness-enhancing design strategies.

5.2.2. Multi-scaled tests

The multiscale tribological evaluation of CBFMs encompasses micron-scale scratch testing of component interfaces, reduced-scaled dynamometer tests using pin-on-disc and ring-on-ring braking systems, and full-scale (1:1) dynamometer testing Fig. 16 [52,68,112–114]. The micron scratch testing and reduced-scaled braking testing discussed above are restricted to evaluating the single-component, bicomponent, and reduced-scale tribological properties of CBFMs, making it challenging to directly extrapolate their properties to practical applications. Therefore, it is essential to accurately evaluate the braking properties of CBFMs, particularly under extreme service conditions. China Railway Corporation designed various braking force testing protocols for different brake pad materials, including CBFM pads, providing reference test results and allowable error margins for each protocol. Simulated experiments conducted under these conditions are referred to as full-scale dynamometer tests [115]. Full-scale dynamometers exhibit high consistency with the actual braking processes of high-speed trains and are a prerequisite for brake pad material approval before installation. With the increasing operating speed of high-speed trains, Full-scale dynamometer tests have become costly and time-consuming due to technical and equipment limitations, making them suitable only for well-established product systems [116].

The structural size effect of reduced-scale dynamometers on test specimens causes significant differences in heat flux and energy conversion, making it challenging to directly evaluate the application of newly developed CBFMs using such devices. This limitation often results in discrepancies between test outcomes from full-scale dynamometer test rigs and small-scale dynamometer experiments. To date, the inherent limitations in the correlation of these testing methods remain unresolved.

5.2.3. Brake disc materials: C/C-SiC instead of cast steel

CBFMs and their counterparts form the friction pair, where the type of counterpart material significantly affects the braking property of CBFMs. To effectively reduce maintenance costs, it is required in engineering to maintain the high stability of CBFMs while minimizing the replacement frequency of counterpart materials. Therefore, under these pairing conditions, CBFMs and their counterparts need to form a well-matched relationship. In the pursuit of increased speed, lightweight design, and safety, steel counterparts are limited by their high density and the tendency to develop thermal cracks due to excessive temperature rise at the friction interface [111] (Fig. 17a), making them inadequate for meeting high-speed and lightweight development needs. C/C-SiC, with its advantages of low density, high wear resistance, and superior thermal shock resistance, is expected to replace traditional steel discs in the coming years. For instance, C/C-SiC paired with CBFMs has been adopted in high-speed trains exceeding 400 km/h (Fig. 17c and d) [117]. The transition to C/C-SiC brake disc materials introduces challenges for existing CBFMs: (i) considerable COF fluctuations at varying braking speeds, resulting in inadequate performance at high speeds (Fig. 17e); (ii) abnormal wear behavior, characterized by a sharp escalation in wear volume with increasing braking speeds (Fig. 17f) [118].

To develop CBFMs mated with C/C-SiC, Chen et al. found that when mated with carbon-ceramic discs, a thicker oxide layer formed on the brake pad surface, enhancing the COF and braking stability while reducing the wear rate [87]. The predominant wear mechanism was oxidative wear. Li et al. reported issues of surface tribo-layer damage and abnormally increased wear when CBFMs interacted with carbon-ceramic discs during high-speed braking [119]. Ma et al. investigated the tribological behavior of powder metallurgy, i.e., carbon-ceramic material systems [120]. Through analyses of wear surfaces and tribo-layer structure, braking property of brake pad materials and inferred differences in wear mechanisms were evaluated. Zhao et al. systematically analyzed the braking behavior of carbon-ceramic composites and CBFMs under both dry and wet braking conditions [121]. The addition of 5 % SiC increased the hardness of CBFMs by over 50 %; however, despite the higher hardness, the wear rate increased by 30 %. Adding graphite lubricant improved the COF by 10 %. The lower hardness of the material increased the actual contact area, allowing it to maintain a low wear rate at high

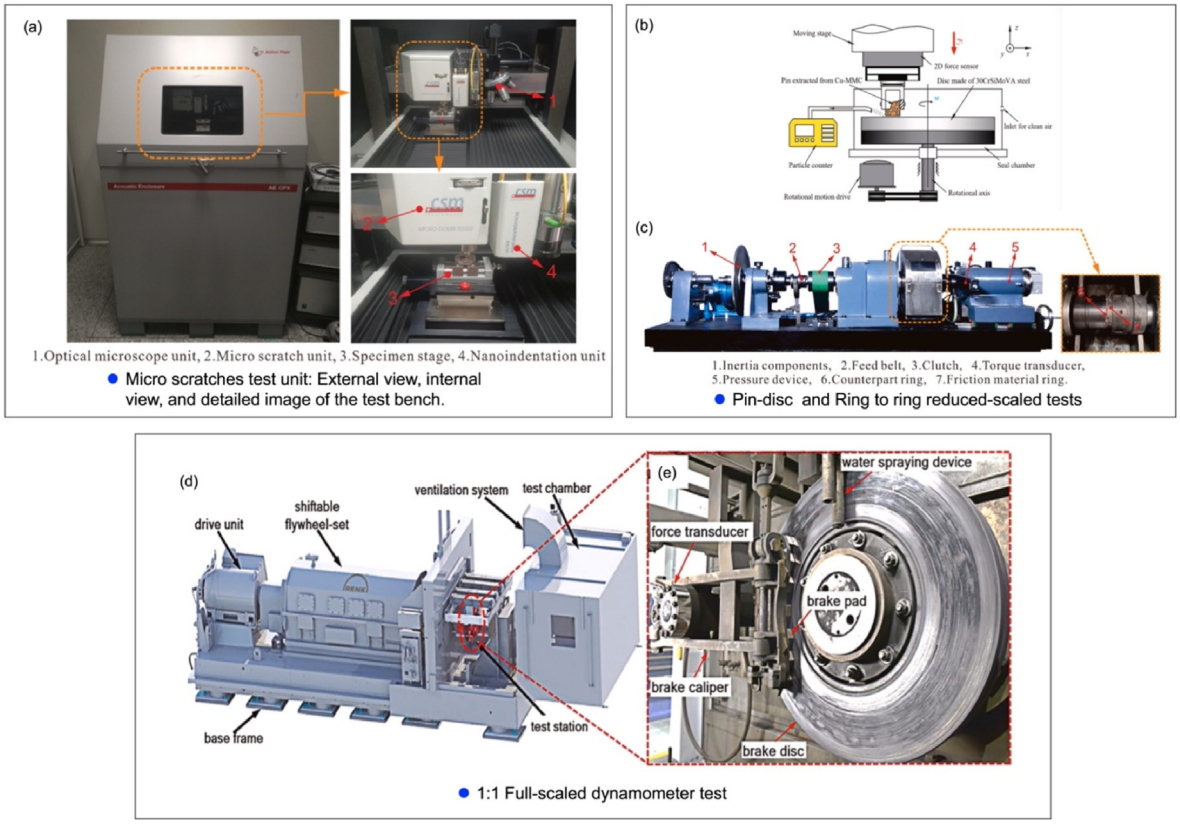

Fig. 16. Multiple scales testers of CBFMs. (a) Mictoscratches test. (b,c) Reduced-scale dynamometer. (d,e) Full-scale dynamometer. Taken from Refs. [26,69,114,116] with permission.

temperatures when mated with C/C-SiC [122].

Substituting cast steel with C/C-SiC discs mated with CBFM brake pads fundamentally transforms contact characteristics, frictional vibrations, and interfacial temperature evolution. Consequently, the friction and wear mechanisms established for high-energy braking in powder metallurgy/steel systems become obsolete, demanding comprehensive reevaluation and further research. This limitation of new CBFMs and wear mechanism can be attributed to several factors: First, the heterogeneous microstructure of C/C-SiC, characterized by carbon fibers oriented along both the *X/Y* and *Z* axes, along with agglomerated CVI-derived carbon and SiC, poses significant challenges for elucidating the wear resistance, stability, and wear mechanisms of CMMCs. The 2.5D woven C/C matrix struggles to maintain a uniform dynamic balance in the wear and regeneration of the counterpart disc during braking, making it difficult to achieve stable braking property with CBFMs. Second, due to the substantial differences in thermal conductivity and higher hardness of C/C-SiC brake discs compared to steel, CBFMs must absorb and dissipate substantial frictional heat under severe conditions, leading to excessive wear. Addressing these issues requires synchronizing the mechanical and thermal properties of C/C-SiC and CBFMs, investigating the tribo-layer evolution under higher-speed braking conditions, and uncovering novel wear mechanisms in the CBFM of C/C-SiC. This is essential to promote their broader applicability.

6. Conclusions and outlook

With the advancement of high-end transportation equipment, significant progress has been made in the application research of CBFMs in braking systems for high-speed trains. (i) Multi-element reinforcement of the matrix and the synergistic interaction of lubricating elements present substantial advantages in optimizing CBFM braking property. Commonly utilized abrasive components include Fe, CrFe, and ZrO_2, with specific functional additives capable of absorbing greater braking energy and facilitating the formation of a nano-ceramic layer, thereby enhancing overall CBFM property. (ii) The interface between frictional and lubricating components and the Cu matrix demonstrates a strong correlation between microscopic tribological behavior and macroscopic braking property. Diffusion-bonded interfaces offer superior adhesion properties, significantly enhancing wear resistance, whereas mechanically bonded interfaces are susceptible to third-body wear and fluctuations in the COF. (iii) Significant advancements have been made in the tribological understanding of pure copper, including mechanisms such as grain reorientation and dislocation-driven plasticity. Owing to the micron-scale differentiation of the tribo-layer, nanoscale qualitative analysis encounters inherent limitations. Conversely, quantitative analysis provides a robust framework for correlating the tribo-layer's microstructure, properties, and macroscopic braking performance. (iv) Open braking systems subject CBFMs to complex and challenging operational environments characterized by high humidity, subzero temperatures, and elevated thermal conditions. Furthermore, as high-speed trains advance toward higher speeds and lightweight designs, C/C-SiC brake discs are poised to replace conventional cast steel, profoundly influencing the design strategies and property optimization of CBFMs.

The challenges remain:

(1) The alloying of the matrix, coupled with the synergistic effects of multiple components, markedly improves the braking property of CBFMs. The strategic design of these components plays a pivotal role in optimizing hardness and thermal conductivity, which are crucial determinants of CBFM's overall properties. While microscale interfacial damage of components provides insights into macroscopic braking performance, establishing a comprehensive correlation between the interfacial properties of these components and the behavior of the tribo-layer under varying braking

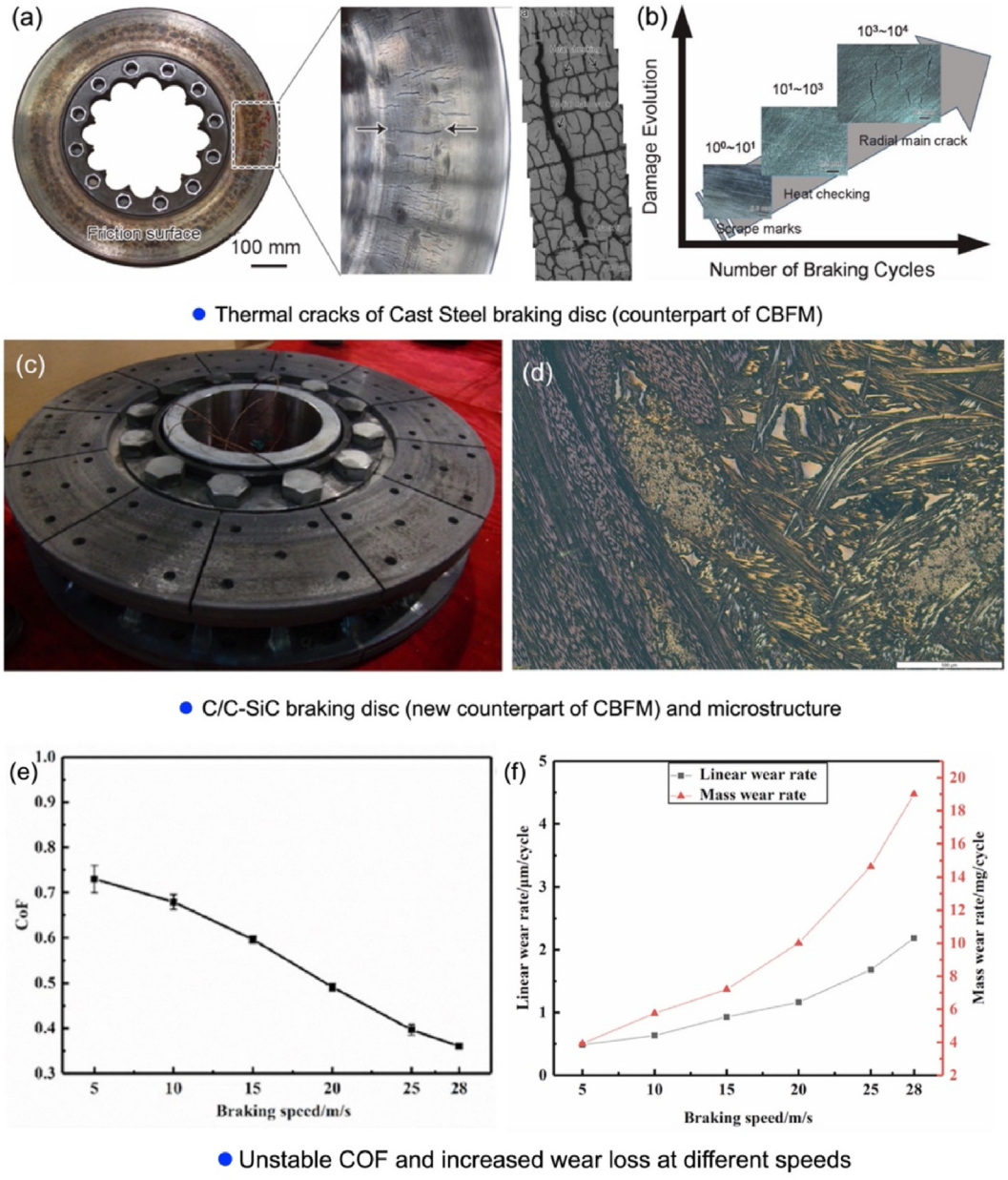

Fig. 17. Different brake discs and brake properties. (a,b) Cast steel brake disc and thermal cracks. (c,d) C/C-SiC brake disc and microstructure. (e,f) COF and wear rate of CBFM when mated with C/C-SiC at different speeds. Taken from Refs. [117,118] with permission.

conditions is essential to accurately elucidate their role in thermo-mechanical coupling scenarios.

(2) The microscopic wear mechanisms at the interface effectively reflect and explain macroscopic braking property characteristics. However, such explanations are challenging to apply to more complex CBFM systems. Discussions on single-component and matrix interfaces need to be extended to the tribological characteristics of multi-component interfaces, revealing the synergistic effects of tribological interfaces at the microscopic level and their correlation with macroscopic braking property. Establishing cross-scale wear mechanisms from microscopic to macroscopic levels will facilitate the development of interface design methods suitable for various braking conditions.

(3) The crystal deformation induced by friction in copper matrices provides a theoretical basis for the transfer of frictional energy on metal surfaces. However, this crystal tribology theory has not been ideally linked to the formation and damage of the tribo-layer evolving on the CBFM surface. Most studies focus on elemental analysis of the tribo-layer surface rather than on deformation mechanisms. Therefore, quantitative research on the formation and damage of the tribo-layer on CBFMs surfaces will be a potential direction for establishing intrinsic links between metal crystal deformation and frictional energy transfer.

(4) The demands for higher speed and lightweight development in high-speed trains place greater requirements on the comprehensive property of CBFMs, as the service environment faces extreme conditions such as rapidly increasing braking energy and exceptionally high braking temperatures. Additionally, the lightweight C/C-SiC brake disc replacing cast steel discs and the comprehensive thermal, mechanical, and tribological compatibility of CBFMs mated with C/C-SiC will be a key focus for future development.

CRediT authorship contribution statement

Yuxuan Xu: Writing – original draft, Methodology, Investigation. **Haibin Zhou:** Investigation, Data curation. **Qi Chen:** Methodology. **Donglin Liu:** Investigation. **Yong Han:** Writing – review & editing. **Minwen Deng:** Methodology. **Pingping Yao:** Writing – review & editing, Supervision, Methodology, Investigation.

Declaration of competing interest

The authors declare that they have no known competing financial interests or personal relationships that could have appeared to influence the work reported in this paper.

Acknowledgments

The authors sincerely acknowledge the financial support from the National Natural Science Foundation of China (52175209, 52205243), and the Natural Science Foundation of Hunan Province (2023JJ057).

References

[1] M. Utsunomiya, K. Hodota, Financial lessons from Asian experience in constructing and operating high-speed train networks, Transportation 38 (2011) 753–764, https://doi.org/10.1007/s11116-011-9348-7.
[2] C.Y. Deng, J. Yin, H.B. Zhang, X. Xiong, P. Wang, M. Sun, The tribological properties of Cf/Cu/C composites under applied electric current, Tribol. Int. 116 (2017) 84–94, https://doi.org/10.1016/j.triboint.2017.07.005.
[3] L. Zhou, Z.Y. Shen, Progress in high-speed train technology around the world, Railway Eng. Sci. 19 (2011) 1–6, https://doi.org/10.1007/bf03325733.
[4] J.K. Xiao, T.T. Li, T.F. Bao, J. Chen, C. Zhang, Oxidation behavior of Cu-based brake pad for high-speed train, Trans. Nonferrous Metals Soc. China 34 (2024) 2260–2274, https://doi.org/10.1016/S1003-6326(24)66539-8.
[5] C.Y. Yu, W.P. Li, Y. Guo, X.B. Sun, F.L. Hong, N. Sun, Q.H. Zhang, Research on wear rate of train brake pads driven by small sample data, Wear 536–537 (2024) 205169, https://doi.org/10.1016/j.wear.2023.205169.
[6] Y.L. Xiao, Z.Y. Zhang, P.P. Yao, K.Y. Fan, H.B. Zhou, T.M. Gong, L. Zhao, M.W. Deng, Mechanical and tribological behaviors of copper metal matrix composites for brake pads used in high-speed trains, Tribol. Int. 119 (2018) 585–592, https://doi.org/10.1016/j.triboint.2017.11.038.
[7] S.Q. Zhao, Q.Z. Yan, T. Peng, X.L. Zhang, Y.Y. Wen, The braking behaviors of Cu-based powder metallurgy brake pads mated with C/C–SiC disk for high-speed train, Wear 448–449 (2020) 203237, https://doi.org/10.1016/j.wear.2020.203237.
[8] H. Kasem, J.F. Brunel, P. Dufrénoy, M. Siroux, B. Desmet, Thermal levels and subsurface damage induced by the occurrence of hot spots during high-energy braking, Wear 270 (2013) 355–364, https://doi.org/10.1016/j.wear.2010.11.007.
[9] R. Mann, V. Magnier, J.F. Brunel, F. Brunel, P. Dufrénoy, M. Henrion, Relation between mechanical behavior and microstructure of a sintered material for braking application, Wear 386–387 (2017) 1–16, https://doi.org/10.1016/j.wear.2017.05.013.
[10] R.T. Liu, J. Chen, X. Xiong, Influence of porogen type and copper powder morphology on property of sintering copper porous materials, J. Cent. South Univ. 25 (2018) 2143–2149, https://doi.org/10.1007/s11771-018-3903-8.
[11] P. Li, C.G. Chen, Q. Qin, T.X. Lu, Y.R. Shao, F. Yang, J.J. Hao, Z.M. Guo, Sintering microstructure and properties of copper powder prepared by electrolyzation and atomization, J. Cent. South Univ. 28 (2021) 1986, https://doi.org/10.1007/s11771-021-4745-3, 1977.
[12] Y.X. Xu, P.Y. Zhou, Q. Chen, H.B. Zhou, M.W. Deng, Y. Han, P.P. Yao, Superior mechanical properties and wear resistance of copper/graphite metallic composites fabricated with fibrous copper powder, Mater. Lett. 368 (2024) 136683, https://doi.org/10.1016/j.matlet.2024.136683.
[13] P. Zhang, L. Zhang, D.B. Wei, X.H. Qu, Effect of matrix alloying on braking performance of copper-based brake pad under continuous emergency braking, J. Tribol. 142 (2020) 081703, https://doi.org/10.1115/1.4046624.
[14] L. Dubourg, H. Pelletier, D. Vaissiere, F. Hlawka, A. Cornet, Mechanical characterisation of laser surface alloyed aluminium–copper systems, Wear 253 (2002) 1077–1085, https://doi.org/10.1016/s0043-1648(02)00218-1.
[15] Y.X. Xu, P.Y. Zhou, Q. Chen, Z.Y. Liu, X. Wang, M.W. Deng, H.B. Zhou, Y. Han, P.P. Yao, The effect of copper particles coated with graphene oxide on tribological properties and tribo-layers of copper metal matrix composites, Tribol. Int. 199 (2024) 110041, https://doi.org/10.1016/j.triboint.2024.110041.
[16] Y. Xian, Z.Y. Zou, C.J. Tu, Y.C. Ding, T.T. Liao, F.C. Zhang, Q. Luo, G.N. Wu, G.Q. Gao, Identifying the effects of cobalt addition in copper-graphene nanoplatelet composites towards improved tribological performance, J. Alloys Compd. 835 (2020) 155444, https://doi.org/10.1016/j.jallcom.2020.155444.
[17] Y. Xian, Z.Y. Zou, C.J. Tu, Y.C. Ding, Y.X. Xu, G.Q. Gao, Direct quantification of the effects of titanium on the copper/graphene interfacial strength, Mater. Lett. 273 (2020) 127969, https://doi.org/10.1016/j.matlet.2020.127969.
[18] R.V. VigneshK, K.R. Kannan, K.V. Shankar, M. Govindaraju, Tribological characteristics of a functionally gradient iron-based wind turbine brake pads reinforced with praseodymium oxide, Emergent Mater 7 (2024) 247–261, https://doi.org/10.1007/s42247-023-00593-x.
[19] R.J. Kasi, N.K. Murugesan, A. Jeyakanapathy, V.V. Ramalingam, G. Myilsamy, Development of functionally gradient Cu-Fe based sintered brake pad materials, Phys. Scripta 99 (2024) 061501, https://doi.org/10.1088/1402-4896/ad4792.
[20] D. Zheng, X. Zhao, K. An, L. Chen, Y. Zhao, D.F. Khan, X.H. Qu, H.Q. Yin, Effects of Fe and graphite on friction and wear properties of brake friction materials for high-speed and heavy-duty vehicles, Tribol. Int. 178 (2023) 108061, https://doi.org/10.1016/j.triboint.2022.108061.
[21] P. Zhang, L. Zhang, K.X. Fu, J.W. Cao, C.R. Shijia, X.H. Qu, Effects of different forms of Fe powder additives on the simulated braking performance of Cu-based friction materials for high-speed railway trains, Wear 414–415 (2018) 317–326, https://doi.org/10.1016/j.wear.2018.09.006.
[22] T. Peng, Q.Z. Yan, G. Li, X.L. Zhang, The influence of Cu/Fe ratio on the tribological behavior of brake friction materials, Tribol. Lett. 66 (2017) 18, https://doi.org/10.1007/s11249-017-0961-2.
[23] W.H. Xu, C.J. Fu, M. Zhong, G.X. Xie, X.Z. Xie, Effect of type and content of iron powder on the formation of oxidized film and tribological properties of Cu-matrix composites, Mater. Des. 214 (2022) 110383, https://doi.org/10.1016/j.matdes.2022.110383.
[24] S. Wu, Q.F. Si, S.L. Pan, J.X. Liu, A.Y. Jiang, J.L. Fan, Y. Li, Y. Wang, Effect of iron powder type on friction and wear properties of copper-based friction powder metallurgy material, Tribol. Trans. 66 (2023) 1019–1025, https://doi.org/10.1080/10402004.2023.2261200.
[25] W.H. Xu, D. Hu, Z.Y. Xu, J.L. Wang, M.R. Yi, M. Zhong, H.H. Wu, M. Huang, Effect of micro/nano carbonyl iron powder on tribological performance of Cu-matrix composites, Tribol. Int. 200 (2024) 107983, https://doi.org/10.1016/j.triboint.2024.110094.
[26] T.M. Gong, P.P. Yao, X. Xiong, H.B. Zhou, Z.Y. Zhang, Y.L. Xiao, L. Zhao, M.W. Deng, Microstructure and tribological behavior of interfaces in Cu-SiO_2 and Cu-Cr metal matrix composites, J. Alloys Compd. 786 (2019) 975–985, https://doi.org/10.1016/j.jallcom.2019.01.255.
[27] H.B. Zhou, P.P. Yao, Y.L. Xiao, K.Y. Fan, T. Gong, L. Zhao, Z.Y. Zhang, M.W. Deng, Y. Li, High energy braking behaviors and tribo-map constructions of Cu metal matrix composites with different Cr volume contents, Wear 496–497 (2022) 204275, https://doi.org/10.1016/j.wear.2022.204275.
[28] H.B. Zhou, P.P. Yao, Y.L. Xiao, K.Y. Fan, T. Gong, L. Zhao, M.W. Deng, Z.Y. Zhang, Influence of ferrochromium type on micro and macro tribology behavior of copper metal matrix composites, Tribol. Int. 184 (2023) 108409, https://doi.org/10.1016/j.triboint.2023.108409.
[29] G.J. Cui, J. Ren, Z.X. Lu, The microstructure and wear characteristics of Cu-Fe matrix friction material with addition of SiC, Tribol. Lett. 65 (2017) 108, https://doi.org/10.1007/s11249-017-0890-0.
[30] Z.Y. Xu, M. Zhong, M.H. Xu, G.X. Xie, H.J. Hu, Effects of aluminosilicate particles on tribological performance and friction mechanism of Cu-matrix pads for high-speed trains, Tribol. Int. 177 (2023) 107983, https://doi.org/10.1016/j.triboint.2022.107983.
[31] L. Zhang, K.X. Fu, P. Zhang, J.W. Cao, C.R. Shijia, Improved braking performance of Cu-based brake pads by utilizing Cu-coated SiO_2 powder, Tribol. Trans. 63 (2020) 829–840, https://doi.org/10.1080/10402004.2020.1754537.
[32] L.N. Si, C. Liu, H.J. Yan, Y.J. Wang, Y. Yang, S.T. Zhang, Y.Y. Zhang, The influences of high temperature on tribological properties of Cu-based friction materials with a friction phase of SiO_2/SiC/Al_2O_3, AIP Adv. 11 (2021) 025335, https://doi.org/10.1063/5.0040220.
[33] T. Peng, Q.Z. Yan, X.L. Zhang, Y. Zhuang, Role of titanium carbide and alumina on the friction increment for Cu-based metallic brake pads under different initial braking speeds, Friction 9 (2021) 1543–1557, https://doi.org/10.1007/s40544-020-0439-3.
[34] J.Q. Wu, Z. Li, G.Y. Wen, Z.L. Gao, Y. Li, P. Xiao, Sepiolite: a new component suitable for 380 km/h high-speed rail brake pads, Adv. Powder Mater. 3 (2024) 100199, https://doi.org/10.1016/j.apmate.2024.100199.
[35] J.Q. Wu, Z. Li, G.Y. Wen, Z.L. Gao, Y. Li, A new wear-resistant component system of copper-based composite materials: modified sepiolite-complex ceramic powder, Ceram. Int. 50 (2024) 18559–18568, https://doi.org/10.1016/j.ceramint.2024.02.340.
[36] J.Q. Wu, Z. Li, Z.L. Gao, G.Y. Wen, Y. Zhao, Y. Li, C. Wu, H. Nie, Analysis of the mechanical, thermal and frictional behavior of Cu-sepiolite composite materials, Appl. Clay Sci. 250 (2024) 107288, https://doi.org/10.1016/j.clay.2024.107288.
[37] J.Q. Wu, Z. Li, G.Y. Wen, H. Liu, Z.L. Gao, Y. Li, Y. Zhao, M. Jin, Structure analysis of friction layer of copper matrix composites reinforced by composite ceramic (TiC-B_4C) powder, Ceram. Int. 49 (2023) 23140–23152, https://doi.org/10.1016/j.ceramint.2023.04.142.
[38] J.Q. Wu, Z. Li, G.Y. Wen, Z.L. Gao, Y. Li, Y. Zhao, Friction mechanism analysis of copper-based composites reinforced with ball-milled and modified composite ceramic powders, Wear (2023) 528–529, https://doi.org/10.1016/j.wear.2023.204959, 204959.
[39] J.Q. Wu, Z. Li, G.Y. Wen, Z.L. Gao, Y. Li, The influence of ceramic powder modification temperature on copper-based composite materials: a perspective on mechanical and frictional behavior, Tribol. Int. 195 (2024) 109642, https://doi.org/10.1016/j.triboint.2024.109642.

[40] J.Q. Wu, Z. Li, Y. Luo, Z.L. Gao, Y. Li, Y. Zhao, Y. Liao, C. Wu, M. Jin, Influence of synergistic strengthening effect of B_4C and TiC on tribological behavior of copper-based powder metallurgy, Ceram. Int. 49 (2023) 2978–2990, https://doi.org/10.1016/j.ceramint.2022.09.282.
[41] S. Gupta, M.W. Barsoum, On the tribology of the MAX phases and their composites during dry sliding: a review, Wear 271 (2011) 1878–1894, https://doi.org/10.1016/j.wear.2011.01.043.
[42] L. Wu, J.X. Chen, M.Y. Liu, Y.W. Bao, Y.C. Zhou, Reciprocating friction and wear behavior of Ti_3AlC_2 and Ti_3AlC_2/Al_2O_3 composites against AISI52100 bearing steel, Wear 266 (2009) 158–166, https://doi.org/10.1016/j.wear.2008.06.009.
[43] J.Q. Ma, F. Li, L.C. Fu, S.Y. Zhu, Z.H. Qiao, J. Yang, W.M. Liu, Effect of counterface on the tribological behavior of Ti_3AlC_2 at ambient, Tribol. Lett. 53 (2014) 311–317, https://doi.org/10.1007/s11249-013-0269-9.
[44] S. Wang, S.Y. Zhu, J. Cheng, Z.H. Qiao, J. Yang, W.M. Liu, Microstructural, mechanical and tribological properties of Al matrix composites reinforced with Cu-coated Ti_3AlC_2, J. Alloys Compd. 690 (2017) 612–620, https://doi.org/10.1016/j.jallcom.2016.08.175.
[45] Z.L. Gao, Z. Li, G.Y. Wen, J.Q. Wu, Y. Li, Y.B. Zhao, M. Jin, Investigation of the tribological mechanisms of TiN-ZrO_2-B_4C ternary ceramic-reinforced copper-metal matrix composites, Tribol. Int. 196 (2024) 109705, https://doi.org/10.1016/j.triboint.2024.109705.
[46] Z.L. Gao, Z. Li, G.Y. Wen, J.Q. Wu, Y. Li, H.Y. Nie, M.T. Wei, Synergistic reinforcement mechanisms of Cu/graphite composites with MAX phase Ti_2AlN and ZrO_2-B_4C ceramics: enhancements in mechanical, thermal, and tribological properties, Ceram. Int. 50 (2024) 48799–48813, https://doi.org/10.1016/j.ceramint.2024.09.234.
[47] W.Q. Lian, Y.J. Mai, J. Wang, L.Y. Zhang, C.S. Liu, X.H. Jie, Fabrication of graphene oxide-Ti_3AlC_2 synergistically reinforced copper matrix composites with enhanced tribological performance, Ceram. Int. 45 (2019) 18592–18598, https://doi.org/10.1016/j.ceramint.2019.06.082.
[48] P. Zhang, L. Zhang, D.B. Wei, P.F. Wu, J.W. Cao, C.R. Shijia, X.H. Qu, K.X. Fu, Effect of graphite type on the contact plateaus and friction properties of copper-based friction material for high-speed railway train, Wear 432 (2019) 202927, https://doi.org/10.1016/j.wear.2019.202927.
[49] J.L. Fan, N.G. Wang, X. Wang, Y.F. Hao, S. Wu, Y. Wang, J.X. Liu, Effect of the coke/flake graphite ratio on the microstructure and properties of Cu-based powder metallurgy friction materials, J. Mater. Eng. Perform. 31 (2022) 10378–10392, https://doi.org/10.1007/s11665-022-06998-9.
[50] Y.X. Xu, D.L. Liu, Q. Chen, P.Y. Zhou, Z.Y. Liu, X. Wang, M.W. Deng, H.B. Zhou, Y. Han, P.P. Yao, Enhanced braking performance of copper metal matrix composites incorporating fine mosaic pitch coke when mated with 30CrMnVA and C/C-SiC, Tribol. Int. 202 (2025) 110378, https://doi.org/10.1016/j.triboint.2024.110378.
[51] X.Y. Lin, R.T. Liu, L. Wang, Z.Z. Li, X. Xiong, N. Liao, J. Chen, The synergistic effect of carbon materials on properties of copper-based friction materials, Ind. Lubric. Tribol. 73 (2021) 170–176, https://doi.org/10.1108/ilt-02-2020-0075.
[52] C.J. Fu, M. Zhong, W.H. Xu, G.X. Xie, H.J. Hu, Synergistic effects of different graphite on the braking performance of Cu-matrix friction materials for high-speed trains based on pin-disc tests, Tribol. Trans. 65 (2022) 1008–1021, https://doi.org/10.1080/10402004.2022.2110344.
[53] X. Zhang, Y.Z. Zhang, S.M. Du, Z.H. Yang, T.T. He, Z. Li, Study on the tribological performance of copper-based powder metallurgical friction materials with Cu-coated or uncoated graphite particles as lubricants, Materials 11 (2018) 2016, https://doi.org/10.3390/ma11102016.
[54] P. Zhang, L. Zhang, D.B. Wei, P.F. Wu, J.W. Cao, C.R. Shijia, X.H. Qu, Adjusting function of MoS_2 on the high-speed emergency braking properties of copper-based brake pad and the analysis of relevant tribo-film of eddy structure, Composites, Part B 185 (2020) 107779, https://doi.org/10.1016/j.compositesb.2020.107779.
[55] T.X. Qiu, S.Y. Pan, C. Fan, X.F. Zhu, X.P. Shen, Effect of Ni-coated MoS_2 on microstructure and tribological properties of (Cu-10Sn)-based composites, Trans. Nonferr. Met. Soc. 30 (2020) 2480–2490, https://doi.org/10.1016/s1003-6326(20)65394-8.
[56] B.M. Chen, Q.L. Bi, J. Yang, Y.Q. Xia, J.C. Hao, Tribological properties of solid lubricants (graphite, h-BN) for Cu-based P/M friction composites, Tribol. Int. 41 (2008) 1145–1152, https://doi.org/10.1016/j.triboint.2008.02.014.
[57] F. Chen, Z. Li, L.F. Zou, W.J. Ma, J.W. Li, Z. Chen, Z.B. Niu, P.F. Liu, P. Xiao, Tribological behavior and mechanism of h-BN modified copper metal matrix composites paired with C/C–SiC, Tribol. Int. 53 (2021) 106561, https://doi.org/10.1016/j.triboint.2020.106561.
[58] M. Freschi, M.D. Virgilio, G. Zanardi, M. Mariani, N. Lecis, G. Dotelli, Employment of micro- and nano-WS_2 structures to enhance the tribological properties of copper matrix composites, Lubricants 9 (2021) 53, https://doi.org/10.3390/lubricants9050053.
[59] P. Zhang, L. Zhang, P.F. Wu, J.W. Cao, C.R. Shijia, D.B. Wei, X.H. Qu, Effect of carbon fiber on the braking performance of copper-based brake pad under continuous high-energy braking conditions, Wear 458 (2020) 203408, https://doi.org/10.1016/j.wear.2020.203408.
[60] Z.Y. Xiang, J.L. Mo, H. Ouyang, F. Massi, B. Tang, Z.R. Zhou, Contact behaviour and vibrational response of a high-speed train brake friction block, Tribol. Int. 152 (2020) 106540, https://doi.org/10.1016/j.triboint.2020.106540.
[61] Y.B. Guo, X.L. Zhou, K. Lee, H.C. Yoon, Q. Xu, D.G. Wang, Recent development in friction of 2D materials: from mechanisms to applications, Nanotechnology 32 (2021) 312002, https://doi.org/10.1088/1361-6528/abfa52.
[62] P. Zhang, L. Zhang, D.B. Wei, P.F. Wu, J.W. Cao, C.R. Shijia, X.H. Qu, A high-performance copper-based brake pad for high-speed railway trains and its surface substance evolution and wear mechanism at high temperature, Wear 444 (2020) 203182, https://doi.org/10.1016/j.wear.2019.203182.
[63] C.C. Chen, Q. Yang, Q.G. Chen, Y.H. Wang, D. Xu, H.Z. Li, X.L. Zhang, C.M. Harvey, J.W. Liu, Tribological properties of copper-embedded self-lubricating bearing materials, Ind. Lubric. Tribol. 74 (2022) 796–803, https://doi.org/10.1108/ilt-03-2022-0067.
[64] A.M. Kovalchenko, O.I. Fushchich, S. Danyluk, The tribological properties and mechanism of wear of Cu-based sintered powder materials containing molybdenum disulfide and molybdenum diselenite under unlubricated sliding against copper, Wear 290–291 (2012) 106–123, https://doi.org/10.1016/j.wear.2012.05.001.
[65] A. Saurabh, P.C. Verma, A. Dhir, J. Sikder, P. Saravanan, S.K. Tiwari, R. Das, Enhanced tribological performance of MoS_2 and hBN-based composite friction materials: design of tribo-pair for automotive brake pad-disc systems, Tribol. Int. 199 (2024) 110001, https://doi.org/10.1016/j.triboint.2024.110001.
[66] Z.Y. Zhang, H.B. Zhou, P.P. Yao, K.Y.H. Fan, Y. Liu, L. Zhao, Y.L. Xiao, T.M. Gong, M.W. Deng, Effect of Fe and Cr on the macro/micro tribological behaviours of copper-based composites, Materials 14 (2021) 3417, https://doi.org/10.3390/ma14123417.
[67] X. Xiong, J. Chen, P.P. Yao, S.P. Li, B.Y. Huang, Friction and wear behaviors and mechanisms of Fe and SiO_2 in Cu-based P/M friction materials, Wear 262 (2007) 1182–1186, https://doi.org/10.1016/j.wear.2006.11.001.
[68] H.H. Zou, X. Ran, W.W. Zhu, Y. Wang, S.Q. Zhan, Z.K. Hao, Tribological behavior of copper–graphite composites reinforced with Cu-coated or uncoated SiO_2 particles, Materials 11 (2018) 2414, https://doi.org/10.3390/ma11122414.
[69] H.B. Zhou, P.P. Yao, T.M. Gong, Y.L. Xiao, Z.Y. Zhang, L. Zhao, K.Y. Fan, M.W. Deng, Effects of ZrO_2 crystal structure on the tribological properties of copper metal matrix composites, Tribol. Int. 138 (2019) 380–391, https://doi.org/10.1016/j.triboint.2019.06.005.
[70] J.K. Xiao, L. Zhang, K.C. Zhou, X.P. Wang, Microscratch behavior of copper–graphite composites, Tribol. Int. 57 (2013) 38–45, https://doi.org/10.1016/j.triboint.2012.07.004.
[71] L. Zhao, P.P. Yao, H.B. Zhou, T.M. Gong, M.W. Deng, Z.Y. Zhang, Y.L. Xiao, H. Deng, Y. Li, F.H. Luo, Effect of CNTs in copper matrix on mechanical characteristics and tribological behavior under dry sliding and boundary lubrication conditions, Materials 12 (2019) 2203, https://doi.org/10.3390/ma12132203.
[72] I. Hutchings, Tribology: friction and wear of engineering materials, Mater. Des. 13 (1992) 187, https://doi.org/10.1016/0261-3069(92)90241-9.
[73] W.M. Rainforth, Microstructural evolution at the worn surface: a comparison of metals and ceramics, Wear 245 (2000) 162–177, https://doi.org/10.1016/s0043-1648(00)00476-2.
[74] D.A. Rigney, R. Divakar, S.M. Kuo, Deformation substructures associated with very large plastic strains, Scripta Metall. Mater. 27 (1992) 975–980, https://doi.org/10.1016/0956-716X(92)90459-R.
[75] C. Greiner, J. Gagel, P. Gumbsch, Solids under extreme shear: friction-mediated subsurface structural transformations, Adv. Mater. 31 (2019) 1806705, https://doi.org/10.1002/adma.201806705.
[76] C. Haug, F. Ruebeling, A. Kashiwar, P. Gumbsch, C. Kübel, C. Greiner, Early deformation mechanisms in the shear-affected region underneath a copper sliding contact, Nat. Commun. 11 (2020) 839, https://doi.org/10.1038/s41467-020-14640-2.
[77] D.A. Rigney, Transfer, mixing and associated chemical and mechanical pro- cesses during the sliding of ductile materials, Wear 245 (1) (2000) 1–9, https://doi.org/10.1016/s0043-1648(00)00460-9.
[78] S.Y. Tarasov, D.V. Lychagin, A.V. Chumaevskii, E.A. Kolubaev, S.A. Belyaev, Subsurface deformation in copper single crystals during reciprocal sliding, Phys. Solid State 54 (2012) 2034–2048, https://doi.org/10.1134/s1063783412100320.
[79] M.A. Meyers, A. Mishra, D.J. Benson, Mechanical properties of nanocrystalline materials, Prog. Mater. Sci. 51 (2006) 427–556, https://doi.org/10.1016/j.pmatsci.2005.08.003.
[80] M. Chen, E. Ma, K.J. Hemker, H. Sheng, Y.M. Wang, X.M. Cheng, Deformation twinning in nanocrystalline aluminum, Science 300 (2003) 1275–1277, https://doi.org/10.1126/science.1083727.
[81] J. Hu, Y.N. Shi, X. Sauvage, G. Sha, K. Lu, Grain boundary stability governs hardening and softening in extremely fine nanograined metals, Science 355 (2017) 1292–1296, https://doi.org/10.1126/science.aal5166.
[82] T. Zhu, J. Li, A. Samanta, A. Leach, K. Gall, Temperature and strain-rate dependence of surface dislocation nucleation, Phys. Rev. Lett. 100 (2008) 025502, https://doi.org/10.1103/PhysRevLett.100.025502.
[83] W.D. Nix, H. Gao, Indentation size effects in crystalline materials: a law for strain gradient plasticity, J. Mech. Phys. Solid. 46 (1998) 411–425, https://doi.org/10.1016/S0022-5096(97)00086-0.
[84] C. Greiner, Z. Liu, R. Schneider, L. Pastewka, P. Gumbsch, The origin of surface microstructure evolution in sliding friction, Scr. Mater. 153 (2018) 63–67, https://doi.org/10.1016/j.scriptamat.2018.04.048.
[85] C. Haug, F. Ruebeling, A. Kashiwar, P. Gumbsch, C. Kübel, C. Greiner, Early deformation mechanisms in the shear-affected region underneath a copper sliding contact, Nat. Commun. 11 (2020) 839, https://doi.org/10.1038/s41467-020-14640-2.
[86] X. Chen, R. Schneider, P. Gumbsch, C. Greiner, Microstructure evolution and deformation mechanisms during high rate and cryogenic sliding of copper, Acta Mater. 161 (2018) 138–149, https://doi.org/10.1016/j.actamat.2018.09.016.
[87] F. Chen, Z. Li, Y. Luo, D.J. Li, W.J. Ma, C. Zhang, H.X. Tang, F. Li, P. Xiao, Braking behaviors of Cu-based PM brake pads mating with C/C-SiC and 30CrMnSi steel

discs under high-energy braking, Wear 486 (2021) 204019, https://doi.org/10.1016/j.wear.2021.204019.
[88] H.B. Zhou, P.P. Yao, Y.L. Xiao, K.Y. Fan, Z.Y. Zhang, T.M. Gong, L. Zhao, M.W. Deng, C. Liu, P. Ling, Friction and wear maps of copper metal matrix composites with different iron volume content, Tribol. Int. 132 (2019) 199–210, https://doi.org/10.1016/j.triboint.2018.11.027.
[89] J.R. Jiang, F.H. Stott, M.M. Stack, The role of triboparticulates in dry sliding wear, Tribol. Int. 31 (1998) 245–256, https://doi.org/10.1016/s0301-679x(98)00027-9.
[90] F.H. Stott, The role of oxidation in the wear of alloys, Tribol. Int. 31 (1998) 61–71, https://doi.org/10.1016/s0301-679x(98)00008-5.
[91] J.E. Mogonye, T.W. Scharf, Tribological properties and mechanisms of self-mated ultrafine-grained titanium, Wear 376–377 (2018) 29–59, https://doi.org/10.1016/j.wear.2016.10.016.
[92] W. Österle, I. Urban, Friction layers and friction films on PMC brake pads, Wear 257 (2004) 215–226, https://doi.org/10.1016/j.wear.2003.12.017.
[93] W. Sawczuk, M.G. Agnieszka, D. Ulbrich, J. Kowalczyk, A.M.R. Cañás, Investigation and modeling of the weight wear of friction pads of a railway disc brake, Materials 15 (2022) 6312, https://doi.org/10.3390/ma15186312.
[94] T. Peng, Q.Z. Yan, G. Li, X.L. Zhang, Z.F. Wen, X.S. Jin, The braking behaviors of Cu-based metallic brake pad for high-speed train under different initial braking speed, Tribol. Lett. 65 (2017) 135, https://doi.org/10.1007/s11249-017-0914-9.
[95] J.K. Xiao, S.X. Xiao, J. Chen, C. Zhang, Wear mechanism of Cu-based brake pad for high-speed train braking at speed of 380 km/h, Tribol. Int. 150 (2020) 106357, https://doi.org/10.1016/j.triboint.2020.106357.
[96] C.H. Yin, Y.L. Liang, Y. Liang, W. Li, M. Yang, Formation of a self-lubricating layer by oxidation and solid-state amorphization of nano-lamellar microstructures during dry sliding wear tests, Acta Mater. 166 (2019) 208–220, https://doi.org/10.1016/j.actamat.2018.12.049.
[97] C.G. Lee, Q.Y. Li, W. Kalb, X.Z. Liu, H. Berger, R.W. Carpick, J. Hone, Frictional characteristics of atomically thin sheets, Science 328 (2010) 76–80, https://doi.org/10.1126/science.1184167.
[98] Y.X. Xu, P.Y. Zhou, Q. Chen, Z.Y. Liu, X. Wang, M.W. Deng, H.B. Zhou, Y. Han, P.P. Yao, Quantitative evolution of tribo-layers in copper based friction materials for high-speed trains operating at 400 km/h equivalent energy density: ratio of formation to damage, Wear (2025) 562–563, https://doi.org/10.1016/j.wear.2024.205678, 205678.
[99] C.E. Morstein, A. Klemenz, M. Dienwiebel, M. Moseler, Humidity-dependent lubrication of highly loaded contacts by graphite and a structural transition to turbostratic carbon, Nat. Commun. 13 (2022) 5958, https://doi.org/10.1038/s41467-022-33481-9.
[100] V.R. Singireddy, R. Jogineedi, S.K. Kancharla, K. Farokhzadeh, P. Filip, On scaled-down bench testing to accelerate the development of novel friction brake materials, Tribol. Int. 174 (2022) 107754, https://doi.org/10.1016/j.triboint.2022.107754.
[101] Y. Desplanques, O. Roussette, G. Degallaix, G. Degallaix, R. Copin, Y. Berthier, Analysis of tribological behaviour of pad-disc contact in railway braking - Part 1. Laboratory test development, compromises between actual and simulated tribological triplets, Wear 262 (2007) 582–591, https://doi.org/10.1016/j.wear.2006.07.004.
[102] Y.L. Xiao, Y. Cheng, M.X. Shen, P.P. Yao, J.H. Du, D.H. Ji, H.P. Zhao, S.P. Liu, L.C. Hua, Friction and wear behavior of copper metal matrix composites at temperatures up to 800°C, J. Mater. Res. Technol. 19 (2022) 2050–2062, https://doi.org/10.1016/j.jmrt.2022.05.192.
[103] P.G. Sanders, T.M. Dalka, R.H. Basch, A reduced-scale brake dynamometer for friction characterization, Tribol. Int. 34 (2001) 609–615, https://doi.org/10.1016/S0301-679X(01)00053-6.
[104] Y.L. Xiao, Y. Cheng, H.B. Zhou, W.H. Liang, M.X. Shen, P.P. Yao, H.P. Zhao, G.Y. Xiong, Evolution of contact surface characteristics and tribological properties of a copper-based sintered material during high-energy braking, Wear 488–489 (2022) 204163, https://doi.org/10.1016/j.wear.2021.204163.
[105] Y. Tabbai, A. Alaoui-Belghiti, R.E. Moznine, F. Belhora, A. Hajjaji, A.E. Ballout, Friction and wear performance of disc brake pads and pyroelectric energy harvesting, Int. J. Precis. Eng. Manuf.-Green Tech. 8 (2021) 487–500, https://doi.org/10.1007/s40684-020-00195-6.
[106] L. Ma, S.Y. Ding, C. Zhang, Y.Z. Huang, X. Zhang, Study on the wear performance of high-speed railway brake materials at low temperatures under continuous braking conditions, Wear 512 (2023) 204556, https://doi.org/10.1016/j.wear.2022.204556.
[107] J.Y. Zuo, X.P. Wang, J.L. Liu, Study on the ice-coated brake disc for EMUs based on force coupling, J. Phys. Conf. Ser. 1986 (2021) 012061, https://doi.org/10.1088/1742-6596/1986/1/012061.
[108] L. Ma, S.Y. Ding, C. Zhang, M.X. Zhang, H.B. Shi, Study on the wear performance of brake materials for high-speed railway with intermittent braking under low-temperature environment conditions, Materials 15 (2022) 8763, https://doi.org/10.3390/ma15248763.
[109] S.Y. Ding, M.X. Zhang, Y.D. Ou, L. Ma, Study on the influence of friction and wear properties of high-speed rail brake materials under humidity environment and temperature conditions, Materials 16 (2023) 1610, https://doi.org/10.3390/ma16041610.
[110] L. Ma, S.Y. Ding, C. Zhang, Y.Z. Huang, X. Zhang, Study on the wear performance of high-speed railway brake materials at low temperatures under continuous braking conditions, Wear (2023) 512–513, https://doi.org/10.1016/j.wear.2022.204556, 204556.
[111] Z.Z. Wang, J.M. Han, J.P. Domblesky, Z.A. Li, X.G. Fan, X.L. Liu, Crack propagation and microstructural transformation on the friction surface of a high-speed railway brake disc, Wear 428 (2019) 45–54, https://doi.org/10.1016/j.wear.2019.01.124.
[112] P.G. Sanders, T.M. Dalka, R.H. Basch, A reduced-scale brake dynamometer for friction characterization, Tribol. Int. 34 (2001) 609–615, https://doi.org/10.1016/s0301-679x(01)00053-6.
[113] C. Octau, D. Meresse, M. Watremez, J. Schiffler, M. Lippert, L. Keirsbulck, L. Dubar, Characterization of particulate matter emissions in urban train braking - an investigation of braking conditions influence on a reduced-scale device, Environ. Sci. Pollut. Res. 27 (2020) 18615–18631, https://doi.org/10.1007/s11356-020-08337-8.
[114] Y. Cheng, Y.L. Xiao, J.H. Du, D.H. Ji, M.X. Shen, Size effect of CrFe particles on tribological behavior and airborne particle emissions of copper metal matrix composites, Tribol. Int. 183 (2023) 108376, https://doi.org/10.1016/j.triboint.2023.108376.
[115] P. Zhang, D.B. Wei, E. Mei, B. Xie, Y.C. Liang, X.Y. Ding, L. Zhang, X.H. Qu, The braking performance and failure mechanism of copper-based brake pads during repeated emergency braking at 400 km/h, Wear (2024) 558–559, https://doi.org/10.1016/j.wear.2024.205532, 205532.
[116] W.G. Zhong, X.H. Zhang, Z.J. Wang, X.L. Zhang, Q.Z. Yan, The braking performance of pads for high-speed train with rigid and flexible structure on a full-scale flywheel brake dynamometer, Tribol. Int. 179 (2023) 108143, https://doi.org/10.1016/j.triboint.2022.108143.
[117] Z. Li, P. Xiao, B.G. Zhang, Y. Li, Y.H. Lu, S.H. Zhu, Preparation and dynamometer tests of 3D needle-punched C/C-SiC composites for high-speed and heavy-Duty brake systems, Int. J. Appl. Ceram. Technol. 13 (2016) 423–433, https://doi.org/10.1111/ijac.12514.
[118] S.W. Fan, H.D. Sun, X. Ma, J.L. Deng, C. Yang, L. Cheng, L.T. Zhang, Microstructure and properties of a new structure-function integrated C/C-SiC brake material, J. Alloys Compd. 769 (2018) 239–249, https://doi.org/10.1016/j.jallcom.2018.07.362.
[119] G. Li, Q.Z. Yan, Comparison of friction and wear behavior between C/C, C/C-SiC and metallic composite materials, Tribol. Lett. 60 (2015) 15, https://doi.org/10.1007/s11249-015-0591-5.
[120] X. Ma, C.H. Luan, S.W. Fan, J.L. Deng, L.T. Zhang, L.F. Cheng, Comparison of braking behaviors between iron- and copper-based powder metallurgy brake pads used for C/C-SiC disc, Tribol. Int. 154 (2021) 106686, https://doi.org/10.1016/j.triboint.2020.106686.
[121] S.Q. Zhao, X.L. Zhang, W.G. Zhong, Y.Y. Wen, Q.Z. Yan, The wet braking and recovery behaviors of the P/M pad mated with C/C–SiC disc for high-speed trains, Wear 468–469 (2021) 203609, https://doi.org/10.1016/j.wear.2020.203609.
[122] Z. tadler, K. Krnel, T. Kosmac, Friction and wear of sintered metallic brake linings on a C/C-SiC composite brake disc, Wear 265 (2008) 278–285, https://doi.org/10.1016/j.wear.2007.10.015.